Journal of Scientific Computing (2021) 87:13
https://doi.org/10.1007/s10915-021-01418-x

Optimal Energy Conserving Local Discontinuous Galerkin Methods for Elastodynamics: Semi and Fully Discrete Error Analysis

Ruchi Guo[1] · **Yulong Xing**[2]

Received: 20 August 2020 / Revised: 7 December 2020 / Accepted: 23 January 2021

Abstract
We present an arbitrary high-order local discontinuous Galerkin (LDG) method with alternating fluxes for solving linear elastodynamics problems in isotropic media. Both the semi-discrete analysis and fully discrete analysis for a leap-frog LDG method are given to show that the proposed method simultaneously enjoys the energy conserving property and optimal convergence rates in both the displacement and stress, when the tensor product polynomials of the degree k are used on Cartesian meshes. Numerical experiments demonstrate that the proposed method has several advantages including the exact energy conservation, slow-growing errors in long time simulation, and subtle dependence on the first Lamé parameter λ.

Keywords Elastodynamics · Elastic wave propagation · Local discontinuous Galerkin methods · Energy conservation · Fully discrete convergence analysis

Mathematics Subject Classification 65N12 · 65N15 · 65N30 · 35Q74 · 74H15 · 74S05

1 Introduction

In this paper, we develop and analyze a local discontinuous Galerkin (LDG) method for the following planar linear elastic wave equations in isotropic media over the time interval $[0, T]$:

$$\rho \mathbf{u}_{tt} - \nabla \cdot \boldsymbol{\sigma}(\mathbf{u}) = \mathbf{f} \quad \text{in } \Omega, \tag{1.1a}$$

Y. Xing: The work of this author is partially supported by the NSF grant DMS-1753581.

✉ Yulong Xing
xing.205@osu.edu

Ruchi Guo
ruchig@uci.edu

[1] Department of Mathematics, University of California Irvine, Irvine, CA 92697, USA

[2] Department of Mathematics, The Ohio State University, Columbus, OH 43210, USA

Published online: 24 February 2021

$$\mathbf{u}(0) = \mathbf{u}_0, \quad \mathbf{u}_t(0) = \mathbf{v}_0, \tag{1.1b}$$

subject to periodic boundary conditions or Dirichlet/Neumann boundary conditions given by

$$\mathbf{u} = \mathbf{g}_D \quad \text{on } \partial\Omega_D \quad \text{and} \quad \boldsymbol{\sigma}(\mathbf{u})\mathbf{n} = \mathbf{g}_N \quad \text{on } \partial\Omega_N, \tag{1.2}$$

with $\overline{\partial\Omega_D} \cup \overline{\partial\Omega_N} = \overline{\partial\Omega}$, where $\mathbf{u}$ represents the displacement of the elastic body $\Omega \subseteq \mathbb{R}^2$ and $\boldsymbol{\sigma}$ is the stress tensor defined as

$$\boldsymbol{\sigma} = \lambda(\nabla \cdot \mathbf{u})\mathbf{I}_2 + 2\mu\boldsymbol{\epsilon}(\mathbf{u}), \quad \text{with the strain tensor: } \boldsymbol{\epsilon}(\mathbf{u}) = \frac{1}{2}(\nabla\mathbf{u} + \nabla\mathbf{u}^T). \tag{1.3}$$

It can be directly verified that the stress and strain tensors have the following relation

$$\boldsymbol{\sigma} = \mathcal{B}\boldsymbol{\epsilon} := \lambda \mathrm{tr}(\boldsymbol{\epsilon})\mathbf{I}_2 + 2\mu\boldsymbol{\epsilon}, \quad \text{and} \quad \boldsymbol{\epsilon} = \mathcal{A}\boldsymbol{\sigma} = \frac{1}{2\mu}\left(\boldsymbol{\sigma} - \frac{\lambda}{2(\lambda+\mu)}\mathrm{tr}(\boldsymbol{\sigma})\mathbf{I}_2\right), \tag{1.4}$$

where λ and μ are referred as Lamé parameters assumed to be constants. In this article, we shall specify the dependence of error bounds on the ratio λ/μ, i.e., analyze the locking phenomenon. In order to facilitate the analysis, we further assume μ is both bounded below from 0 and above from ∞, and thus restrict the estimate mainly to λ. We also note that large heterogeneity ratios of μ do not correspond to physically relevant situations [19]. Without loss of generality, in the following discussion we assume $\rho = 1$ and $\mathbf{f} = \mathbf{0}$, and all the results are readily extendable to the more general case.

The present research is motivated by wide applications of linear elastodynamics in many practical problems including mechanic engineering, civil engineering, geophysics, biological simulation and so on. Especially it is of critical importance in a variety of inverse problems for non-destructive testing. For example, some medical imaging techniques like elastography [29] require accurate simulation of wave propagation through human bodies where it is more accurately modeled by elastic wave in bone [28]. Another example, seismic inversion, uses elastic waves propagating within the Earth or along its surface to detect oil or gas field [44].

A large variety of numerical methods have been proposed for elastic wave propagation problems. For example, finite difference methods have been widely used in computational elastodynamics [46,50]. The application of finite element methods (FEMs) can be found in [34] for space-time FEMs, [4,6,21,26] for mixed FEMs and [47] for CutFEMs focusing on elastodynamics with multiple material. We also refer readers to the spectral method in [36] as a high-order method. In this paper we focus on discontinuous Galerkin (DG) methods due to their flexibility for higher-order spatial approximation and *hp*-adaptivity, scalability for parallel computation and reduced dispersion errors. In general, there are two groups of methods to tackle second-order wave equations. Methods in the first group rewrite the equation into a system of first order hyperbolic equations, then one can apply the standard DG [15], the interior penalty DG (IPDG) [43], the nodal DG [31], the hybridizable DG (HDG) [42], the space-time DG [24] and the stagger DG [12] methods for examples. For elastic wave equations, methods in this group use the velocity–stress and velocity–strain formulation in general. The second group deals with the second order derivative directly, see the IPDG [54], and the LDG methods to be discussed in this paper. The displacement-stress and displacement–strain formulations for elastic wave equations widely appear in this group. We also refer readers to [35] for a comparison of these two groups of methods including their applications to different wave propagation problems, analysis and numerical methods.

There have been extensive studies on DG methods for the linear elastic wave equation in isotropic media (1.1) over the last decade. For instance, the authors in [55] studied a

high-order DG method for the acoustic–elastic wave propagation problems in terms of a velocity–strain formulation as well as its parallel implementation. Some hp-adaptive DG methods can be found in [18,23,40]. In [11] the authors proposed a staggered DG method for the velocity–stress formulation which can conserve the energy exactly and avoid locking namely the error bound is independent of λ, and they also gave both the semi-discrete and fully discrete analysis. In [3] an energy-based DG method is developed and applied to some realistic problems. The authors in [1] studied DG methods for displacement-stress and displacement formulation with different fluxes. An IPDG method was studied for quasistatic linear viscoelasticity in [43] where both the semi-discrete and fully discrete analysis are presented. We also refer readers to [2,17] and the reference therein for the dispersion analysis of IPDG methods for elastic wave equations. In addition, the authors in [49] studied a HDG method with a velocity-strain formulation for heterogeneous media. A high-order HDG method and its super-convergence properties were investigated in [42]. Some new analysis techniques were proposed in [22] for HDG on elasticity which can lead to the optimal error bound in a simple and concise manner. We also refer readers to [25] for a review of HDG methods on elasticity and elastodynamics.

LDG methods can be traced back to [16] as the generalization of the standard DG method in [5] to solve Navier–Stokes problems. The basic idea is to apply the standard DG discretization to a mixed formulation of the underling partial differential equations (PDEs). We refer readers to [8,57] and the references therein for various applications of LDG methods such as elliptic problems, convection-diffusion problems, the dispersive equations, and so on. Recently, there have been many studies in designing DG and LDG methods which can numerically preserve the energy or Hamiltonian structure of the model in the discrete level, which can lead to small phase and shape errors in long time simulations. Energy conserving LDG methods have been designed for the generalized Korteweg-de Vries equation [7], the acoustic wave equation [10,13,56], the Degasperis–Procesi equation [32], the Camassa–Holm equation [39], the nonlinear Schrödinger equation [38], the improved Boussinesq equation [37] and so on.

Usually it is challenging to obtain DG methods for wave equations which are both non-dissipative (i.e., energy conserving for the physical energy) and have (provable) optimal high order accuracy at the same time. In [10,56], Xing, Chou and Shu proposed an LDG method for the second order wave equation in the 1D and 2D cases such that the physical energy can be exactly conserved. Semi-discrete analysis is also given to show that the LDG method has the optimal convergence rate. In this paper, we consider the linear elastic wave equations (1.1) and propose an optimal energy conserving LDG method. The proposed method has several remarkable advantages. First, fully discrete error analysis is carried out to demonstrate that it has arbitrary high-order optimal convergence rates in both displacement and stress tensor. Second, it can exactly conserve the energy in the discrete level. Comparison of the numerical performance of the proposed LDG method and an IPDG method is also provided to demonstrate the excellent behavior of energy conserving methods in long time simulation. The third one is the independence of the solution error of displacement with respect to the first Lamé parameter λ, which is a desired property for numerical solvers of elastodynamics.

One of the major difficulties of this research lies on the approximation for the stress or strain which is a symmetric tensor. For the issue of symmetry in elasticity, we refer readers to [6,21] for the strong enforcement and [4] for the weak enforcement. In the proposed method, the piecewise tensor product polynomials of the degree k, denoted by $\mathbb{Q}^k$, are used for approximation in which the symmetry of the stress tensor is strongly enforced. Then the key obscure part in the analysis is a suitable choice of the projection operator for the stress tensor such that it can both maintain the symmetry and handle the penalty terms on element edges. We refer readers to [20,51,58] for various construction of projection operators with

different purposes in the analysis of LDG methods. The one used in this work is based on the Gauss-Radau projection such that the resulted tensor is also symmetric. However special attention should be paid to the extra terms induced by this projection on element edges due to the penalties of the LDG method for which some new super-convergence properties of the Gauss-Radau projection will be established.

We also note that the proposed method can be considered as a special case of the DG methods in [1] with the alternating fluxes and without stability terms. In [1], both LDG and IPDG methods were tested and $O(h^k)$ convergence rate was observed on triangular meshes. In the present work, by choosing a special initial condition constructed by the Gauss-Radau projection, we analytically proved and numerically validated the optimal $O(h^{k+1})$ convergence rate for the displacement and stress, if the polynomial space $\mathbb{Q}^k$ are used on Cartesian meshes. Both theoretical analysis and numerical results indicate this choice of the initial condition is critical for the LDG method to produce the optimal convergent solutions. We also remark that the analytical result in [1] is provided on arbitrary meshes, while the optimal error analysis of LDG methods in this paper is proven for the special Cartesian meshes. It would be interesting to investigate the optimal error estimate of LDG method with generalized fluxes for elastodynamics on unstructured meshes, following the recent work in [48] for the acoustic wave equation.

Another contribution of this paper is the fully discrete error analysis for a second-order leap-frog LDG method. Current analysis for time discretization of LDG methods in the literature are mainly concentrated on the equations with the first-order time derivative, see [51,52,58] and the references therein. Those techniques can not be directly applied to the second-order wave equations, and thus new fundamental estimates are demanded. The fully discrete analysis for the leap-frog IPDG method can be found in [27] for the second order acoustic wave equation, and it employs the elliptic projector induced from the coercive bilinear form of the IPDG method which is not available for the LDG method. By providing some new estimates, we are able to perform detailed analysis to show the dependence of the time step $\triangle t$ on the mesh size h and the polynomial degree k to ensure either the stability or the optimal convergence rate $O(h^{k+1} + \triangle t^2)$. The proposed analysis approach for the fully discrete scheme can be also readily applied to the LDG methods for the second order wave equations in the scalar case [10,56].

This paper consists of six additional sections. In the next section, we introduce some basic notations and develop the LDG method for (1.1). In Sect. 3, we prepare some fundamental identities and estimates which will be frequently used throughout this paper. In Sect. 4, we present the semi-discrete error analysis. In Sect. 5, the fully discrete convergence analysis is given. In Sect. 6, we present a group of numerical examples to demonstrate the features of the proposed method. Some conclusion remarks are provided in Sect. 7.

2 Local Discontinuous Galerkin Scheme

In this section, we introduce some basic notations and derive the LDG scheme for the equations of elastodynamics (1.1). We only consider the rectangular domain $\Omega \subseteq \mathbb{R}^2$, and for simplicity we let $\Omega = [0, L_1] \times [0, L_2]$ in analysis. Although only the 2D situation is considered in this paper, we emphasize that the proposed method and the analysis techniques are readily extendable to the 3D Cartesian meshes since all the elements and projection operators are constructed by tensor products. Denote $H^k(\omega)$ and $W^{k,p}(0, T; H^k(\omega))$ as the standard Hilbert spaces and Sobolev spaces with temporal dimension, defined on a subdomain $\omega \subseteq \Omega$

with periodic boundary conditions on Ω. In the following discussion, for each vector function $\mathbf{v}$ we always assume $\mathbf{v} = [v_1, v_2]^T$ is a column vector with the superscript "T" denoting the transpose, $\nabla v_i = [\partial_{x_1} v_i, \partial_{x_2} v_i]$, $i = 1, 2$ is a row vector and $\nabla \mathbf{v} = \begin{bmatrix} \nabla v_1 \\ \nabla v_2 \end{bmatrix}$ is a 2-by-2 tensor. We employ the notation ":" such that $\boldsymbol{\tau}^1 : \boldsymbol{\tau}^2 = \sum_{i,j=1}^2 \tau_{ij}^1 \tau_{ij}^2$ for any two tensors $\boldsymbol{\tau}^1 = \left[\tau_{ij}^1\right]_{i,j=1}^2$ and $\boldsymbol{\tau}^2 = \left[\tau_{ij}^2\right]_{i,j=1}^2$. Throughout this paper, C denotes a generic positive constant independent of λ, spatial and temporal step sizes h and Δt, which may have different values at different occasions and may depend on μ, $\bar{\mu}$.

Let $\mathcal{T}_h$ be a Cartesian mesh of Ω; namely we cut Ω into $N_1 \times N_2$ rectangular elements in which N_i denotes the partition in the x_i direction, $i = 1, 2$. Define $h_i = L_i/N_i$, $i = 1, 2$. We assume the mesh $\mathcal{T}_h$ is shape regular, i.e., there exist constants c and C such that $c \le h_1/h_2 \le C$. Let $\mathcal{E}_h^i$ and $\mathcal{E}_h^b$ be the interior and boundary edges, respectively; and let $\mathcal{E}_h = \mathcal{E}_h^i \cup \mathcal{E}_h^b$. On this mesh $\mathcal{T}_h$, we introduce the following broken polynomial spaces:

$$\mathbf{V}_h^k = \{\mathbf{v}_h \ : \ \mathbf{v}_h|_K \in [\mathbb{Q}^k(K)]^2, \ \ \forall K \in \mathcal{T}_h\},$$
$$\boldsymbol{\Sigma}_h^k = \{\boldsymbol{\tau}_h \ : \ \boldsymbol{\tau}_h|_K \in [\mathbb{Q}^k(K)]^{2\times 2}, \ \ \boldsymbol{\tau}_h^T = \boldsymbol{\tau}_h, \ \ \forall K \in \mathcal{T}_h\},$$

where $\mathbb{Q}^k(K)$ is the space of tensor product of one-dimensional polynomials with degree no more than k. Note that the symmetry of the stress tensor is incorporated in the piecewise polynomial space $\boldsymbol{\Sigma}_h^k$. For each edge $e \in \mathcal{E}_h^i$, we let K_e^- and K_e^+ be the elements below and above e if e is horizontal, or be the elements left and right to e if e is vertical. By this set up, for each $\mathbf{v}_h \in \mathbf{V}_h^k$, we define $\mathbf{v}_h^{\pm}|_e = (\mathbf{v}_{K_e^{\pm}})|_e$, namely the limit values of $\mathbf{v}_h$ at e from the left/bottom elements or from the right/top elements, respectively. Similarly, we can define $\boldsymbol{\tau}_h^{\pm}|_e$. Note that if $e \in \mathcal{E}_h^b$, we employ the same notation, but the related neighbor elements outside the domain are then defined as the corresponding elements on the other side of the domain due to periodic boundary conditions. Also, we define $(\cdot, \cdot)_\omega$ as the standard L^2 inner product over any subdomain $\omega \subseteq \Omega$.

Based on these preparations, we now proceed to derive the LDG method for the Eq. (1.1). For this purpose, we rewrite (1.1a) in the mixed formulation:

$$\mathbf{u}_{tt} - \nabla \cdot \boldsymbol{\sigma} = \mathbf{f}, \tag{2.1a}$$
$$\mathcal{A}\boldsymbol{\sigma} = \frac{1}{2}(\nabla \mathbf{u} + \nabla \mathbf{u}^T). \tag{2.1b}$$

Multiplying (2.1a) by $\mathbf{v}_h \in \mathbf{V}_h^k$ and using the integration by parts on every K, we have

$$\int_K \mathbf{u}_{tt} \cdot \mathbf{v}_h dX - \int_K (\nabla \cdot \boldsymbol{\sigma}) \cdot \mathbf{v}_h dX = \int_K \mathbf{u}_{tt} \cdot \mathbf{v}_h dX + \int_K (\nabla \mathbf{v}_h) : \boldsymbol{\sigma} dX - \int_{\partial K} \mathbf{v}_h^T \boldsymbol{\sigma} \mathbf{n} ds = 0. \tag{2.2}$$

Similarly, multiplying (2.1b) by $\boldsymbol{\tau}_h \in \boldsymbol{\Sigma}_h^k$, applying integration by parts on each element K and using the symmetry of $\boldsymbol{\tau}_h$, we have

$$\int_K \mathcal{A}\boldsymbol{\sigma} : \boldsymbol{\tau}_h = \int_K -(\nabla \cdot \boldsymbol{\tau}_h) \cdot \mathbf{u} dX + \int_{\partial K} \mathbf{u}^T \boldsymbol{\tau}_h \mathbf{n} ds. \tag{2.3}$$

Then we introduce the following bilinear forms for any $\mathbf{v} \in \left[H^1(K)\right]^2$ and symmetric $\boldsymbol{\tau} \in \left[H^1(K)\right]^{2\times 2}$:

$$a_K(\boldsymbol{\tau}, \mathbf{v}) = \int_K (\nabla \mathbf{v}) : \boldsymbol{\tau} dX, \quad b_K(\boldsymbol{\tau}, \mathbf{v}) = \int_K (\nabla \cdot \boldsymbol{\tau}) \cdot \mathbf{v} dX, \quad c_K(\boldsymbol{\tau}, \mathbf{v}) = \int_{\partial K} \mathbf{v}^T \boldsymbol{\tau} \mathbf{n} ds, \tag{2.4}$$

and the corresponding bilinear forms on the whole domain:

$$\begin{aligned} a_h(\boldsymbol{\tau}, \mathbf{v}) &= \sum_{K \in \mathcal{T}_h} \int_K (\nabla \mathbf{v}) : \boldsymbol{\tau} dX, \quad b_h(\boldsymbol{\tau}, \mathbf{v}) = \sum_{K \in \mathcal{T}_h} \int_K (\nabla \cdot \boldsymbol{\tau}) \cdot \mathbf{v} dX, \\ c_h(\boldsymbol{\tau}, \mathbf{v}) &= \sum_{K \in \mathcal{T}_h} \int_{\partial K} \mathbf{v}^T \boldsymbol{\tau} \mathbf{n} ds, \quad \mathring{c}_h(\boldsymbol{\tau}, \mathbf{v}) = c_h(\boldsymbol{\tau}, \mathbf{v}) - \int_{\partial \Omega} \mathbf{v}^T \boldsymbol{\tau} \mathbf{n} ds, \end{aligned} \tag{2.5}$$

where $\mathring{c}_h$ includes only the contribution from the interior edges and excludes the boundary terms. For the case of periodic boundary conditions, the proposed LDG method is to find $\mathbf{u}_h \in \mathbf{V}_h^k$ and $\boldsymbol{\sigma}_h \in \boldsymbol{\Sigma}_h^k$ such that

$$((\mathbf{u}_h)_{tt}, \mathbf{v}_h)_\Omega + a_h(\boldsymbol{\sigma}_h, \mathbf{v}_h) - c_h(\hat{\boldsymbol{\sigma}}_h, \mathbf{v}_h) = 0 \qquad \forall \mathbf{v}_h \in \mathbf{V}_h^k, \tag{2.6a}$$

$$(\mathcal{A}\boldsymbol{\sigma}_h, \boldsymbol{\tau}_h)_\Omega + b_h(\boldsymbol{\tau}_h, \mathbf{u}_h) - c_h(\boldsymbol{\tau}_h, \hat{\mathbf{u}}_h) = 0 \qquad \forall \boldsymbol{\tau}_h \in \boldsymbol{\Sigma}_h^k, \tag{2.6b}$$

where the hatted terms $\hat{\boldsymbol{\sigma}}_h$ and $\hat{\mathbf{u}}_h$ are the so called the numerical fluxes defined on edges. In this paper, we shall consider the simple alternating fluxes:

$$\hat{\boldsymbol{\sigma}}_h = \boldsymbol{\sigma}_h^+, \quad \hat{\mathbf{u}}_h = \mathbf{u}_h^-, \quad \text{or} \quad \hat{\boldsymbol{\sigma}}_h = \boldsymbol{\sigma}_h^-, \quad \hat{\mathbf{u}}_h = \mathbf{u}_h^+. \tag{2.7}$$

Without loss of generality, we shall focus on the first two in (2.7) in this paper. One can also define a family of numerical fluxes as:

$$\hat{\boldsymbol{\sigma}}_h = \alpha \boldsymbol{\sigma}_h^+ + (1-\alpha)\boldsymbol{\sigma}_h^-, \quad \hat{\mathbf{u}}_h = (1-\alpha)\mathbf{u}_h^+ + \alpha \mathbf{u}_h^- \quad \alpha \in [0,\ 1], \tag{2.8}$$

which are the generalization of the alternating fluxes (2.7) (when $\alpha = 0$ or 1) as studied in [41]. This family of numerical fluxes can also be shown to produce energy conserving LDG methods. The optimal error estimate based on this general family may be obtained via the introduction of more sophisticated global projection as studied in [41] for one dimensional problem, and will be explored elsewhere. We also refer readers to [1] for studies on the DG methods with these fluxes on elastodynamics.

Now we recall the Gauss-Radau projection [10,14,20] in order to handle the initial conditions and also for the convergence analysis. Consider an interval $I_i = [x_1^{i-\frac{1}{2}}, x_1^{i+\frac{1}{2}}]$, then a one-dimensional projection operator $P_1^\pm : H^{k+1}(I_i) \to \mathbb{P}^k(I_i)$ is defined as

$$\begin{aligned} &(P_1^\pm w, v)_{I_i} = (w, v)_{I_i}, \quad \forall v \in \mathbb{P}^{k-1}(I_i), \quad \text{and} \\ &P_1^+ w(x_1^{i-\frac{1}{2}}) = w(x_1^{i-\frac{1}{2}}) \text{ or } P_1^- w(x_1^{i+\frac{1}{2}}) = w(x_1^{i+\frac{1}{2}}). \end{aligned} \tag{2.9}$$

Similarly, we can define the projection $P_2^\pm$ on an interval J_j in the x_2 direction. Then a two-dimensional projection operator $P^\pm$ on a rectangle $K_{ij} = I_i \otimes J_j$ is defined as a tensor product $P^\pm := P_1^\pm \otimes P_2^\pm$. The optimal approximation results of $P^\pm$ for scalar functions $w \in H^{k+1}(K)$ can be found in [14,20], i.e.,

$$\|w - P^\pm w\|_{L^2(K)} \le C h^{k+1} \|w\|_{H^{k+1}(K)}. \tag{2.10}$$

Moreover, we can define projection operators for vector and tensor spaces: $\mathbf{P}^\pm : \left[H^{k+1}(K_{ij})\right]^2 \to \left[\mathbb{Q}^k(K_{ij})\right]^2$ and $\boldsymbol{\Pi}^\pm : \left[H^{k+1}(K_{ij})\right]^{2\times 2} \to \left[\mathbb{Q}^k(K_{ij})\right]^{2\times 2}$ such that

$$\mathbf{P}^{\pm}\mathbf{v} = \begin{bmatrix} P^{\pm}v_1 \\ P^{\pm}v_2 \end{bmatrix}, \quad \forall\, \mathbf{v} = \begin{bmatrix} v_1 \\ v_2 \end{bmatrix}, \quad \text{and} \quad \mathbf{\Pi}^{\pm}\boldsymbol{\tau} = \begin{bmatrix} P^{\pm}\tau_{11} & P^{\pm}\tau_{12} \\ P^{\pm}\tau_{21} & P^{\pm}\tau_{22} \end{bmatrix} \quad \forall\, \boldsymbol{\tau} = \begin{bmatrix} \tau_{11} & \tau_{12} \\ \tau_{12} & \tau_{22} \end{bmatrix}. \tag{2.11}$$

Applying (2.10) to each entry of the matrices in (2.11), we have that for each element $K \in \mathcal{T}_h$ and any $\mathbf{v} \in \left[H^{k+1}(K)\right]^2$ and $\boldsymbol{\tau} \in \left[H^{k+1}(K)\right]^{2\times 2}$, there holds

$$\|\mathbf{v} - \mathbf{P}^{\pm}\mathbf{v}\|_{L^2(K)} \le Ch^{k+1}\|\mathbf{v}\|_{H^{k+1}(K)} \quad \text{and} \quad \|\boldsymbol{\tau} - \mathbf{\Pi}^{\pm}\boldsymbol{\tau}\|_{L^2(K)} \le Ch^{k+1}\|\boldsymbol{\tau}\|_{H^{k+1}(K)}, \tag{2.12}$$

where C is a constant only depending on the geometry of the mesh. Now, we can choose the initial conditions to the LDG method (2.6) as

$$\mathbf{u}_h(0) = \mathbf{P}^{-}\mathbf{u}_0 \quad \text{and} \quad (\mathbf{u}_h(0))_t = \mathbf{P}^{-}\mathbf{v}_0 = \mathbf{P}^{-}\mathbf{u}_t(0). \tag{2.13}$$

Without causing any confusion, the variable in "$(\cdot)$" only denotes time, and we ignore the spatial variables. Here we emphasize that the super-script "$-$" should be consistent with the choice of the numerical fluxes in (2.7).

Finally, we introduce the following norms for tensor functions $\boldsymbol{\sigma}, \boldsymbol{\epsilon} \in \left[L^2(\omega)\right]^{2\times 2}$, defined on a subdomain $\omega \subseteq \Omega$:

$$\|\boldsymbol{\sigma}\|^2_{\mathcal{A},\omega} = \int_{\omega} \mathcal{A}\boldsymbol{\sigma} : \boldsymbol{\sigma}\, dX, \quad \text{and} \quad \|\boldsymbol{\epsilon}\|^2_{\mathcal{B},\omega} = \int_{\omega} \mathcal{B}\boldsymbol{\epsilon} : \boldsymbol{\epsilon}\, dX. \tag{2.14}$$

Define the potential energy density as

$$G(\mathbf{u}) = \frac{\lambda}{2}(\nabla \cdot \mathbf{u})^2 + \mu\boldsymbol{\epsilon}(\mathbf{u}) : \boldsymbol{\epsilon}(\mathbf{u}) = \frac{1}{2}\mathcal{A}\boldsymbol{\sigma} : \boldsymbol{\sigma}, \tag{2.15}$$

then the total energy corresponding to the elastodynamics is defined as the integration of the kinetic and potential energy over the whole domain:

$$E(t) = \int_{\Omega} \frac{1}{2}\mathbf{u}_t^2 + G(\mathbf{u})dX = \frac{1}{2}\left(\|\mathbf{u}_t\|^2_{L^2(\Omega)} + \|\boldsymbol{\sigma}\|^2_{\mathcal{A},\Omega}\right). \tag{2.16}$$

It is well known that the total energy in (2.16) will be conserved during the dynamics if traction free, homogeneous Dirichlet or periodic boundary conditions are imposed for which we refer readers to [3] for the derivation. One of the advantages of the proposed LDG method is to exactly conserve this energy in the discrete level.

Remark 2.1 When the Dirichlet boundary condition or Neumann boundary conditions are given, we need to slightly modify the numerical fluxes on the boundary. To describe the modification, we denote the left and bottom boundary by $\partial\Omega^-$ and the right and top boundary by $\partial\Omega^+$. When the Dirichlet boundary condition, say $\mathbf{u} = \mathbf{g}_D$, is given, we keep the numerical fluxes $\mathbf{u}_h^-$ and $\boldsymbol{\sigma}_h^+$ on $\partial\Omega^-$ unchanged, but change them to $\mathbf{u}_h^+$ and $\boldsymbol{\sigma}_h^-$ on $\partial\Omega^+$. Thus we have the boundary integration $\int_{\partial\Omega\cap\partial\Omega_D} \hat{\mathbf{u}}_h^T\boldsymbol{\tau}_h\mathbf{n}ds = \int_{\partial\Omega\cap\partial\Omega_D} \mathbf{g}_D^T\boldsymbol{\tau}_h\mathbf{n}ds$ in (2.6b), which can be moved to the right hand side of the resulting linear system. Similarly, if the Neumann boundary condition $\boldsymbol{\sigma} = \mathbf{g}_N$ is imposed, we keep $\mathbf{u}_h^-$ and $\boldsymbol{\sigma}_h^+$ on $\partial\Omega^+$ unchanged but flip them to $\mathbf{u}_h^+$ and $\boldsymbol{\sigma}_h^-$ on $\partial\Omega^-$. It leads to the boundary integration $\int_{\partial\Omega\cap\partial\Omega_N} \mathbf{v}_h^T\hat{\boldsymbol{\sigma}}_h\mathbf{n}ds = \int_{\partial\Omega\cap\partial\Omega_N} \mathbf{v}_h^T\mathbf{g}_N ds$ moved to the right hand side of (2.6a). This approach can also be applied to handle the mixed type boundary conditions. In a summary, we can take the numerical fluxes on boundary to be

$$\begin{aligned} &\hat{\boldsymbol{\sigma}}_h = \boldsymbol{\sigma}_h = \boldsymbol{\sigma}_h^{\mp} \quad \text{on} \quad \partial\Omega_D \cap \partial\Omega^{\pm}, \quad \hat{\boldsymbol{\sigma}}_h = \boldsymbol{\sigma}_h^{\pm} \quad \text{on} \quad \partial\Omega_N \cap \partial\Omega^{\pm}, \\ &\hat{\mathbf{u}}_h = \mathbf{u}_h^{\pm} \quad \text{on} \quad \partial\Omega_D \cap \partial\Omega^{\pm}, \quad \hat{\mathbf{u}}_h = \mathbf{u}_h = \hat{\mathbf{u}}_h^{\mp} \quad \text{on} \quad \partial\Omega_N \cap \partial\Omega^{\pm}. \end{aligned}$$

Thus, the proposed LDG method for the mixed boundary condition is to find $\mathbf{u}_h \in \mathbf{V}_h^k$ and $\boldsymbol{\sigma}_h \in \boldsymbol{\Sigma}_h^k$ such that

$$((\mathbf{u}_h)_{tt}, \mathbf{v}_h)_\Omega + a_h(\boldsymbol{\sigma}_h, \mathbf{v}_h) - \mathring{c}_h(\hat{\boldsymbol{\sigma}}_h, \mathbf{v}_h) - \int_{\partial\Omega_D} \mathbf{v}_h^T \hat{\boldsymbol{\sigma}}_h \mathbf{n} ds - \int_{\partial\Omega_N} \mathbf{v}_h^T \mathbf{g}_N ds = 0 \qquad \forall \mathbf{v}_h^T \in \mathbf{V}_h^k, \tag{2.17a}$$

$$(\mathcal{A}\boldsymbol{\sigma}_h, \boldsymbol{\tau}_h)_\Omega + b_h(\boldsymbol{\tau}_h, \mathbf{u}_h) - \mathring{c}_h(\boldsymbol{\tau}_h, \hat{\mathbf{u}}_h) - \int_{\partial\Omega_D} \mathbf{g}_D^T \boldsymbol{\tau}_h \mathbf{n} ds - \int_{\partial\Omega_N} \hat{\mathbf{u}}_h^T \boldsymbol{\tau}_h \mathbf{n} ds = 0 \qquad \forall \boldsymbol{\tau}_h \in \boldsymbol{\Sigma}_h^k. \tag{2.17b}$$

3 Some Preliminary Estimates

In this section, we recall and prepare a group of fundamental estimates and identities which will be frequently used in the analysis of this paper. We begin with the following norm equivalence and identities.

Lemma 3.1 *For any tensor* $\boldsymbol{\tau} \in \left[L^2(\omega)\right]^{2\times 2}$ *with* ω *being a subdomain of* Ω*, there holds*

$$\sqrt{2\mu}\|\boldsymbol{\tau}\|_{\mathcal{A},\omega} \le \|\boldsymbol{\tau}\|_{L^2(\omega)} \le \sqrt{2(\lambda+\mu)}\|\boldsymbol{\tau}\|_{\mathcal{A},\omega} \tag{3.1}$$

Proof Using the second identity in (1.4) and the inequality $(\mathrm{tr}(\boldsymbol{\tau}))^2 \le 2(\tau_{11}^2 + \tau_{22}^2) \le 2\|\tau\|^2$, we have

$$\begin{aligned}\|\boldsymbol{\tau}\|_{\mathcal{A},\omega}^2 = \int_\omega \mathcal{A}\boldsymbol{\tau} : \boldsymbol{\tau} dX &= \frac{1}{2\mu}\left(\int_\omega \boldsymbol{\tau}^2 dX - \frac{\lambda}{2(\lambda+\mu)}\int_\omega (\mathrm{tr}(\boldsymbol{\tau}))^2 dX\right) \\ &\ge \frac{1}{2(\lambda+\mu)}\|\boldsymbol{\tau}\|_{L^2(\omega)}^2\end{aligned}$$

which yields the right hand side of (3.1). Using the identity again, we have

$$\|\boldsymbol{\tau}\|_{\mathcal{A},\omega}^2 = \int_\omega \mathcal{A}\boldsymbol{\tau} : \boldsymbol{\tau} dX = \frac{1}{2\mu}\left(\int_\omega \boldsymbol{\tau}^2 dX - \frac{\lambda}{2(\lambda+\mu)}\int_\omega \mathrm{tr}(\boldsymbol{\tau}))^2 dX\right) \le \frac{1}{2\mu}\|\tau\|_{L^2(\omega)}^2$$

which yields the left hand side of (3.1). □

Lemma 3.2 *For any tensor polynomials* $\mathbf{v}_h \in \mathbf{V}_h^k$ *and* $\boldsymbol{\tau}_h \in \boldsymbol{\Sigma}_h^k$*, there holds*

$$a_h(\boldsymbol{\tau}_h, \mathbf{v}_h) + b_h(\boldsymbol{\tau}_h, \mathbf{v}_h) - c_h((\boldsymbol{\tau}_h)^+, \mathbf{v}_h) - c_h(\boldsymbol{\tau}_h, (\mathbf{v}_h)^-) = 0, \tag{3.2a}$$

$$c_h(\boldsymbol{\tau}_h, \mathbf{v}_h) - c_h((\boldsymbol{\tau}_h)^+, \mathbf{v}_h) - c_h(\boldsymbol{\tau}_h, (\mathbf{v}_h)^-) = 0. \tag{3.2b}$$

Proof First, on each element K, the integration by parts yields $a_K(\boldsymbol{\tau}_h, \mathbf{v}_h) = -b_K(\boldsymbol{\tau}_h, \mathbf{v}_h) + c_K(\boldsymbol{\tau}_h, \mathbf{v}_h)$. Therefore, (3.2a) is actually equivalent to (3.2b), and thus we only need to prove (3.2b). We consider one edge $e \in \mathcal{E}_h$. The contributions of all the terms in (3.2b) on this edge e is

$$\int_e (\mathbf{v}_h^T)^- \boldsymbol{\tau}_h^- \mathbf{n} - (\mathbf{v}_h^T)^+ \boldsymbol{\tau}_h^+ \mathbf{n} - (\mathbf{v}_h^T)^+ \boldsymbol{\tau}_h^- \mathbf{n} + (\mathbf{v}_h^T)^+ \boldsymbol{\tau}_h^+ \mathbf{n} - (\mathbf{v}_h^T)^- \boldsymbol{\tau}_h^- \mathbf{n} + (\mathbf{v}_h^T)^+ \boldsymbol{\tau}_h^- \mathbf{n} ds = 0. \tag{3.3}$$

Summing (3.3) yields (3.2b), and this finishes the proof. □

Now, we present a group of super-convergence properties of the projections $\boldsymbol{\Pi}^+$ and $\mathbf{P}^-$.

Lemma 3.3 *There exists a constant C such that for each element K and any $\mathbf{v} \in \left[H^{k+2}(\Omega)\right]^2$, $\boldsymbol{\tau} \in \left[H^{k+2}(\Omega)\right]^{2\times 2}$,*

$$|b_K(\boldsymbol{\tau}_h, \mathbf{v} - \mathbf{P}^-\mathbf{v}) - c_K(\boldsymbol{\tau}_h, (\mathbf{v} - \mathbf{P}^-\mathbf{v})^-)| \le Ch^{k+1}\|\mathbf{v}\|_{H^{k+2}(K)}\|\boldsymbol{\tau}_h\|_{L^2(K)}, \quad \forall \boldsymbol{\tau}_h \in \boldsymbol{\Sigma}_h^k, \tag{3.4a}$$

$$|a_K(\boldsymbol{\tau} - \boldsymbol{\Pi}^+\boldsymbol{\tau}, \mathbf{v}_h) - c_K((\boldsymbol{\tau} - \boldsymbol{\Pi}^+\boldsymbol{\tau})^+, \mathbf{v}_h)| \le Ch^{k+1}\|\boldsymbol{\tau}\|_{H^{k+2}(K)}\|\mathbf{v}_h\|_{L^2(K)}, \quad \forall \mathbf{v}_h \in \mathbf{V}_h^k. \tag{3.4b}$$

Proof We note that (3.4a) directly follows from the property (3.3) of [10] or Lemma 3.6 of [14]. Here we only show (3.4b), and the argument is similar to Lemma 3.6 of [14]. Let $\mathbf{v}_h = \left[v_{h,1}, v_{h,2}\right]^T$ and $\boldsymbol{\tau} = [\boldsymbol{\tau}_1, \boldsymbol{\tau}_2]^T$ with column vectors $\boldsymbol{\tau}_{h,i} = [\tau_{i1}, \tau_{i2}]^T$, $i = 1, 2$. For each $K \in \mathcal{T}_h$, $\mathbf{q} = [q_1, q_2]^T \in \left[H^{k+1}(K)\right]^2$ and $v \in \mathbb{Q}^k(K)$, we define the following functional

$$D_K^+(\mathbf{q}, v) = \int_K \nabla v \cdot (\mathbf{q} - \mathbf{P}^+\mathbf{q})dX - \int_{\partial K} v(\mathbf{q} - (\mathbf{P}^+\mathbf{q})^+) \cdot \mathbf{n}ds. \tag{3.5}$$

We can easily see

$$a_K(\boldsymbol{\tau} - \boldsymbol{\Pi}^+\boldsymbol{\tau}, \mathbf{v}_h) - c_K((\boldsymbol{\tau} - \boldsymbol{\Pi}^+\boldsymbol{\tau})^+, \mathbf{v}_h) = D_K^+(\boldsymbol{\tau}_1, v_{h,1}) + D_K^+(\boldsymbol{\tau}_2, v_{h,2}), \tag{3.6}$$

since $\boldsymbol{\tau}$ is symmetric. Let e_1^b and e_1^t be the bottom and top edges of K in the x_1 direction, and similarly let e_2^b and e_2^t be the right and left edges of K in the x_2 direction. Then, by the definition of $\mathbf{P}^+$ and $P^+ = P_1^+ \otimes P_2^+$, we actually have the following decomposition

$$D_K^+(\boldsymbol{\tau}_i, v_{h,i}) = D_K^1(\tau_{i1}, v_{h,i}) + D_K^2(\tau_{i2}, v_{h,i}), \quad i = 1, 2, \tag{3.7}$$

in which $D_K^l(q, v), l = 1, 2$ are defined locally:

$$\begin{aligned} D_K^1(q, v) &= \int_K \partial_{x_1} v(q - P^+q)dX - \int_{e_2^b \cup e_2^t} v(q - P_2^+q)n_1 dx_2, \quad D_K^2(q, v) \\ &= \int_K \partial_{x_2} v(q - P^+q)dX - \int_{e_1^b \cup e_1^t} v(q - P_1^+q)n_2 dx_1, \end{aligned}$$

where $n_1 = 1$ on e_2^t, $n_1 = -1$ on e_2^b and $n_2 = 1$ on e_1^t, $n_2 = -1$ on e_1^b.

Now, let's consider the reference element $\hat{K} = (-1, 1) \times (-1, 1)$. We proceed to prove

$$D_{\hat{K}}^l(\hat{q}, \hat{v}) = 0, \quad l = 1, 2, \quad \forall \hat{q} \in \mathbb{P}^{k+1}(\hat{K}), \hat{v} \in \mathbb{Q}^k(\hat{K}). \tag{3.8}$$

Without loss of generality, we only show (3.8) for $l = 1$. Since $\mathbf{P}^+$ is $\mathbb{Q}^k$-polynomial preserving, we know that (3.8) is true for $\hat{q} \in \mathbb{Q}^k(\hat{K})$, and thus we only need to show it for $\hat{q} = \hat{x}_1^{k+1}$ and $\hat{x}_2^{k+1}$. First, for $\hat{q} = \hat{x}_1^{k+1}$, since $\partial_{\hat{x}_1}\hat{v}$ is a polynomial with the degree at most $k - 1$, we have $\int_{\hat{K}} \partial_{\hat{x}_1} v(\hat{q} - P^+\hat{q})d\hat{X} = \int_{\hat{K}} \partial_{\hat{x}_1} v(\hat{x}_1^{k+1} - P_1^+\hat{x}_1^{k+1})d\hat{x}_1 d\hat{x}_2 = 0$. Besides, on $\hat{e}_2^b \cup \hat{e}_2^t$, due to $\hat{q} = \hat{x}_1^{k+1}$, we clearly have $P_2^+\hat{q} = \hat{q}$. Therefore, $D_{\hat{K}}^1(\hat{x}_1^{k+1}, \hat{v}) = 0$ for each $v \in \mathbb{Q}^k(\hat{K})$. Second, for $\hat{q} = \hat{x}_2^{k+1}$, we apply integration by parts to the first term in $D_{\hat{K}}^1$ and obtain $D_{\hat{K}}^1(\hat{q}, \hat{v}) = -\int_{\hat{K}} \hat{v}\partial_{\hat{x}_1}(\hat{q} - P^+\hat{q})d\hat{X}$. Clearly $\partial_{\hat{x}_1}(\hat{x}_2^{k+1} - P^+\hat{x}_2^{k+1}) = 0$. Thus, $D_{\hat{K}}^1(\hat{x}_2^{k+1}, \hat{v}) = 0$ for each $\hat{v} \in \mathbb{Q}^k(\hat{K})$ which finishes the proof of (3.8).

Then, on $\hat{K}$, by inverse and trace inequalities, we have $|D_{\hat{K}}^l(\hat{q}, \hat{v})| \le C\|\hat{v}\|_{L^2(\hat{K})}\|\hat{q}\|_{H^{k+2}(\hat{K})}$, $l = 1, 2$, $\forall \hat{q} \in \left[H^{k+2}(\hat{K})\right]^2$. Since $D_{\hat{K}}^l(\hat{q}, \hat{v})$ vanishes on $\left[\mathbb{P}^{k+1}(\hat{K})\right]^2$, the

Bramble–Hilbert lemma further yields

$$|D^l_{\hat{K}}(\hat{q},\hat{v})| \le C\|\hat{v}\|_{L^2(\hat{K})}|\hat{q}|_{H^{k+2}(\hat{K})}, \quad l=1,2. \tag{3.9}$$

Thus, for each $K=(x_1^{i-1/2},x_1^{i+1/2})\times(x_2^{j-1/2},x_2^{j+1/2})$ with $h_1=x_1^{i+1/2}-x_1^{i-1/2}$ and $h_2=x_2^{j+1/2}-x_2^{j-1/2}$, the affine mapping from $\hat{K}$ to K yields $D^+_K(\mathbf{q},v)=h_2D^1_{\hat{K}}(\hat{q}_1,\hat{v})+h_1D^2_{\hat{K}}(\hat{q}_2,\hat{v})$. Using (3.9), we obtain

$$\begin{aligned} D^+_K(\mathbf{q},v) &\le h_2|D^1_{\hat{K}}(\hat{q}_1,\hat{v})|+h_1|D^2_{\hat{K}}(\hat{q}_2,\hat{v})| \\ &\le Ch\|\hat{v}\|_{L^2(\hat{K})}|\hat{\mathbf{q}}|_{H^{k+2}(\hat{K})} \le Ch^{k+1}\|v\|_{L^2(K)}|\mathbf{q}|_{H^{k+2}(K)} \end{aligned}$$

Combining this with (3.6), we obtain the desired result. □

4 The Semi-discrete Method: Energy Conservation and Error Estimate

In this section, we analyze the semi-discrete LDG scheme (2.6). We begin with the energy conservation property for the total energy defined in (2.16). We denote the continuous energy of the elastodynamics by

$$E_h(t)=\int_\Omega \frac{1}{2}(\mathbf{u}_h)_t^2+G(\mathbf{u}_h)dX=\frac{1}{2}\left(\|(\mathbf{u}_h)_t\|^2_{L^2(\Omega)}+\|\boldsymbol{\sigma}_h\|^2_{\mathcal{A},\Omega}\right), \tag{4.1}$$

and proceed to prove the following energy conservation and stability results.

Theorem 4.1 *If the periodic boundary condition is imposed, the continuous energy of the numerical solutions of the LDG scheme (2.6) is conserved for all the time.*

Proof First, putting $\mathbf{u}_h$ and $\boldsymbol{\sigma}_h$ into (2.16) and differentiating it with respect to time, we have

$$E_h'(t)=\int_\Omega (\mathbf{u}_h)_t\cdot(\mathbf{u}_h)_{tt}+\mathcal{A}(\boldsymbol{\sigma}_h)_t:\boldsymbol{\sigma}_h dX. \tag{4.2}$$

For the second term in the right side of (4.2), we take temporal derivative of (2.6b) and choose the test function $\boldsymbol{\tau}_h=\boldsymbol{\sigma}_h$, which leads to

$$((\mathcal{A}\boldsymbol{\sigma}_h)_t,\boldsymbol{\sigma}_h)_\Omega+b_h(\boldsymbol{\sigma}_h,(\mathbf{u}_h)_t)-c_h(\boldsymbol{\sigma}_h,(\mathbf{u}_h^-)_t)=0.$$

For the first term in the right side of (4.2), we test (2.6a) by the $\mathbf{v}_h=(\mathbf{u}_h)_t$ and have

$$((\mathbf{u}_h)_{tt},(\mathbf{u}_h)_t)_\Omega+a_h(\boldsymbol{\sigma}_h,(\mathbf{u}_h)_t)-c_h(\boldsymbol{\sigma}_h^+,(\mathbf{u}_h)_t)=0.$$

We add the two identities above to obtain

$$E_h'(t)=-b_h(\boldsymbol{\sigma}_h,(\mathbf{u}_h)_t)+c_h(\boldsymbol{\sigma}_h,(\mathbf{u}_h^-)_t)-a_h(\boldsymbol{\sigma}_h,(\mathbf{u}_h)_t)+c_h(\boldsymbol{\sigma}_h^+,(\mathbf{u}_h)_t) \tag{4.3}$$

which vanishes due to Lemma 3.2. □

Remark 4.1 The above analysis focuses on the periodic boundary condition, which could also be viewed as the analysis on the interior domain. The stability analysis for the case of mixed boundary conditions is more complicated. For the mixed boundary conditions, taking temporal derivative of (2.17b) and letting $\mathbf{v}_h=(\mathbf{u}_h)_t$ in (2.17a) we obtain

$$((\mathcal{A}\boldsymbol{\sigma}_h)_t,\boldsymbol{\sigma}_h)_\Omega+b_h(\boldsymbol{\sigma}_h,(\mathbf{u}_h)_t)-\mathring{c}_h(\boldsymbol{\sigma}_h,(\hat{\mathbf{u}}_h)_t)-\int_{\partial\Omega_D}(\mathbf{g}_D^T)_t\boldsymbol{\sigma}_h\mathbf{n}ds-\int_{\partial\Omega_N}(\hat{\mathbf{u}}_h^T)_t\boldsymbol{\sigma}_h\mathbf{n}ds=0,$$

$$((\mathbf{u}_h)_{tt},(\mathbf{u}_h)_t)_\Omega+a_h(\boldsymbol{\sigma}_h,(\mathbf{u}_h)_t)-\mathring{c}_h(\hat{\boldsymbol{\sigma}}_h,(\mathbf{u}_h)_t)-\int_{\partial\Omega_D}(\mathbf{u}_h)_t^T\hat{\boldsymbol{\sigma}}_h\mathbf{n}ds-\int_{\partial\Omega_N}(\mathbf{u}_h)_t^T\mathbf{g}_N ds=0.$$

Adding these two identities together, we note all the edge terms cancel with each other due to (3.3). So we have

$$\begin{aligned} E_h'(t) &= -\int_{\partial\Omega} (\mathbf{u}_h)_t^T \boldsymbol{\sigma}_h \mathbf{n} ds + \int_{\partial\Omega_D} (\mathbf{u}_h)_t^T \boldsymbol{\sigma}_h \mathbf{n} ds + \int_{\partial\Omega_N} (\mathbf{u}_h)_t^T \mathbf{g}_N ds + \int_{\partial\Omega_D} (\mathbf{g}_D)_t^T \boldsymbol{\sigma}_h \mathbf{n} ds \\ &\quad + \int_{\partial\Omega_N} (\mathbf{u}_h)_t^T \boldsymbol{\sigma}_h \mathbf{n} ds \\ &= \int_{\partial\Omega_N} (\mathbf{u}_h)_t^T \mathbf{g}_N ds + \int_{\partial\Omega_D} (\mathbf{g}_D)_t^T \boldsymbol{\sigma}_h \mathbf{n} ds, \end{aligned} \tag{4.4}$$

and $E_h'(t) = 0$ if $\mathbf{g}_D = \mathbf{g}_N = \mathbf{0}$. Namely, for the homogeneous mixed boundary conditions, the energy conservation property also holds, and so does the stability. In addition, by the homogenization techniques, the stability also holds for the pure Dirichlet boundary conditions. However, if the mixed boundary condition is imposed and either of $\mathbf{g}_D$ or $\mathbf{g}_N$ is non-zero, the situation becomes complicated. Integrating (4.4) from 0 to T we can obtain the energy identity involving the energy transfer on the boundary

$$E_h(T) = E_h(0) + \int_0^T \int_{\partial\Omega_N} (\mathbf{u}_h)_t^T \mathbf{g}_N ds\, dt + \int_0^T \int_{\partial\Omega_D} (\mathbf{g}_D)_t^T \boldsymbol{\sigma}_h \mathbf{n} ds\, dt. \tag{4.5}$$

A similar identity can be also found in [42] for acoustic wave equations. In [1], a stabilization term was added to the numerical fluxes so that one could bound the boundary terms on the right side of (4.5) and obtain the stability.

In the following discussion on the error analysis, we shall focus on the interior domain and consider the periodic boundary condition. The analysis for the mixed boundary conditions will be left for future research. In order to estimate the semi-discrete solution errors, we decompose the errors in the following way:

$$e_{\mathbf{u}} = \mathbf{u} - \mathbf{u}_h = \eta_{\mathbf{u}} + \xi_{\mathbf{u}}, \qquad \text{where} \quad \eta_{\mathbf{u}} = \mathbf{u} - \mathbf{P}^- \mathbf{u}, \quad \xi_{\mathbf{u}} = \mathbf{P}^- \mathbf{u} - \mathbf{u}_h, \tag{4.6a}$$

$$e_{\boldsymbol{\sigma}} = \boldsymbol{\sigma} - \boldsymbol{\sigma}_h = \eta_{\boldsymbol{\sigma}} + \xi_{\boldsymbol{\sigma}}, \qquad \text{where} \quad \eta_{\boldsymbol{\sigma}} = \boldsymbol{\sigma} - \boldsymbol{\Pi}^+ \boldsymbol{\sigma}, \quad \xi_{\boldsymbol{\sigma}} = \boldsymbol{\Pi}^+ \boldsymbol{\sigma} - \boldsymbol{\sigma}_h. \tag{4.6b}$$

We first show some estimates related to the chosen initial conditions (2.13).

Lemma 4.1 *Under the initial conditions* (2.13) *with* $\boldsymbol{\sigma}_0 = \boldsymbol{\sigma}(\mathbf{u}_0)$, *the following estimates hold*

$$\xi_{\mathbf{u}}(0) = 0, \quad \textit{and} \quad (\xi_{\mathbf{u}})_t(0) = 0, \tag{4.7a}$$

$$\|\xi_{\boldsymbol{\sigma}}(0)\|_{\mathcal{A},\Omega} \le C\sqrt{\lambda+\mu}\big(\|\boldsymbol{\sigma}_0\|_{H^{k+1}(\Omega)} + \|\mathbf{u}_0\|_{H^{k+2}(\Omega)}\big)h^{k+1}. \tag{4.7b}$$

Proof The two terms in (4.7a) directly follow from the definition in (2.13). Now we proceed to analyze (4.7b). We subtract the LDG scheme (2.6b) from the one for the exact solutions, and then write the following equation

$$(\mathcal{A}e_{\boldsymbol{\sigma}}, \boldsymbol{\tau}_h)_\Omega + b_h(\boldsymbol{\tau}_h, e_{\mathbf{u}}) - c_h(\boldsymbol{\tau}_h, e_{\mathbf{u}}^-) = 0, \tag{4.8}$$

at $t = 0$. The super-convergence property (3.4a) yields $\forall \boldsymbol{\tau}_h \in \boldsymbol{\Sigma}_h^k$

$$\begin{aligned} (\mathcal{A}e_{\boldsymbol{\sigma}}, \boldsymbol{\tau}_h)_\Omega &= -b_h(\boldsymbol{\tau}_h, e_{\mathbf{u}}) + c_h(\boldsymbol{\tau}_h, e_{\mathbf{u}}^-) = -b_h(\boldsymbol{\tau}_h, \eta_{\mathbf{u}}) + c_h(\boldsymbol{\tau}_h, \eta_{\mathbf{u}}^-) \\ &\le Ch^{k+1}\|\mathbf{u}_0\|_{H^{k+2}(\Omega)}\|\boldsymbol{\tau}_h\|_{L^2(\Omega)}. \end{aligned} \tag{4.9}$$

Applying the decomposition $e_{\boldsymbol{\sigma}} = \eta_{\boldsymbol{\sigma}} + \xi_{\boldsymbol{\sigma}}$, the approximation (2.12) and norm equivalence (3.1), we obtain

$$\begin{aligned}(\mathcal{A}\xi_{\boldsymbol{\sigma}}, \boldsymbol{\tau}_h)_\Omega &\le -(\mathcal{A}\eta_{\boldsymbol{\sigma}}, \boldsymbol{\tau}_h)_\Omega + Ch^{k+1}\|\mathbf{u}_0\|_{H^{k+2}(\Omega)}\|\boldsymbol{\tau}_h\|_{L^2(\Omega)} \\ &\le \frac{1}{2\mu}\|\eta_{\boldsymbol{\sigma}}\|_{L^2(\Omega)}\|\boldsymbol{\tau}_h\|_{L^2(\Omega)} + Ch^{k+1}\|\mathbf{u}_0\|_{H^{k+2}(\Omega)}\|\boldsymbol{\tau}_h\|_{L^2(\Omega)} \\ &\le Ch^{k+1}\left(\|\boldsymbol{\sigma}_0\|_{H^{k+1}(\Omega)} + \|\mathbf{u}_0\|_{H^{k+2}(\Omega)}\right)\|\boldsymbol{\tau}_h\|_{L^2(\Omega)}.\end{aligned} \tag{4.10}$$

Taking $\boldsymbol{\tau}_h = \xi_{\boldsymbol{\sigma}}$ and using the norm equivalence (3.1), we have

$$\|\xi_{\boldsymbol{\sigma}}\|_{\mathcal{A},\Omega} \le C\sqrt{\lambda+\mu}\big(\|\boldsymbol{\sigma}_0\|_{H^{k+1}(\Omega)} + \|\mathbf{u}_0\|_{H^{k+2}(\Omega)}\big)h^{k+1}. \tag{4.11}$$

□

Next, we show the following optimal error estimate in the energy norm.

Theorem 4.2 *Under the initial conditions* (2.13)*, at any time t the following estimates hold*

$$\|(e_{\mathbf{u}})_t\|_{L^2(\Omega)} \le C\sqrt{\lambda+\mu}\left(\|\mathbf{u}\|_{W^{1,\infty}(0,T;H^{k+2}(\Omega))} + \|\boldsymbol{\sigma}\|_{W^{1,\infty}(0,T;H^{k+2}(\Omega))}\right)h^{k+1}(t+1), \tag{4.12a}$$

$$\|e_{\boldsymbol{\sigma}}\|_{\mathcal{A},\Omega} \le C\sqrt{\lambda+\mu}\left(\|\mathbf{u}\|_{W^{1,\infty}(0,T;H^{k+2}(\Omega))} + \|\boldsymbol{\sigma}\|_{W^{1,\infty}(0,T;H^{k+2}(\Omega))}\right)h^{k+1}(t+1). \tag{4.12b}$$

Proof First of all, since the exact solutions $\mathbf{u}$ and $\boldsymbol{\sigma}$ satisfy the weak form (2.6), we have

$$((e_{\mathbf{u}})_{tt}, \mathbf{v}_h)_\Omega + a_h(e_{\boldsymbol{\sigma}}, \mathbf{v}_h) - c_h(e_{\boldsymbol{\sigma}}^+, \mathbf{v}_h) = 0, \qquad \forall \mathbf{v}_h \in \mathbf{V}_h^k, \tag{4.13a}$$

$$(\mathcal{A}e_{\boldsymbol{\sigma}}, \boldsymbol{\tau}_h)_\Omega + b_h(\boldsymbol{\tau}_h, e_{\mathbf{u}}) - c_h(\boldsymbol{\tau}_h, e_{\mathbf{u}}^-) = 0, \qquad \forall \boldsymbol{\tau}_h \in \mathbf{W}_h^k. \tag{4.13b}$$

Using the decomposition (4.6), we obtain

$$((\xi_{\mathbf{u}})_{tt}, \mathbf{v}_h)_\Omega + ((\eta_{\mathbf{u}})_{tt}, \mathbf{v}_h)_\Omega + a_h(\xi_{\boldsymbol{\sigma}}, \mathbf{v}_h) + a_h(\eta_{\boldsymbol{\sigma}}, \mathbf{v}_h) - c_h(\xi_{\boldsymbol{\sigma}}^+, \mathbf{v}_h) - c_h(\eta_{\boldsymbol{\sigma}}^+, \mathbf{v}_h) = 0, \tag{4.14a}$$

$$(\mathcal{A}\eta_{\boldsymbol{\sigma}}, \boldsymbol{\tau}_h)_\Omega + (\mathcal{A}\xi_{\boldsymbol{\sigma}}, \boldsymbol{\tau}_h)_\Omega + b_h(\boldsymbol{\tau}_h, \eta_{\mathbf{u}}) + b_h(\boldsymbol{\tau}_h, \xi_{\mathbf{u}}) - c_h(\boldsymbol{\tau}_h, \eta_{\mathbf{u}}^-) - c_h(\boldsymbol{\tau}_h, \xi_{\mathbf{u}}^-) = 0. \tag{4.14b}$$

Consider the two equations in (4.14). Taking the time derivative of (4.14b), choosing the test function $\mathbf{v}_h = (\xi_{\mathbf{u}})_t$, $\boldsymbol{\tau}_h = \xi_{\boldsymbol{\sigma}}$ respectively, and then adding the resulted two equations together, we obtain

$$\begin{aligned}&((\xi_{\mathbf{u}})_{tt}, (\xi_{\mathbf{u}})_t)_\Omega + ((\eta_{\mathbf{u}})_{tt}, (\xi_{\mathbf{u}})_t)_\Omega + ((\mathcal{A}\eta_{\boldsymbol{\sigma}})_t, \xi_{\boldsymbol{\sigma}})_\Omega + ((\mathcal{A}\xi_{\boldsymbol{\sigma}})_t, \xi_{\boldsymbol{\sigma}})_\Omega \\ &\quad = -a_h(\xi_{\boldsymbol{\sigma}}, (\xi_{\mathbf{u}})_t) + c_h(\xi_{\boldsymbol{\sigma}}^+, (\xi_{\mathbf{u}})_t) - b_h(\xi_{\boldsymbol{\sigma}}, (\xi_{\mathbf{u}})_t) + c_h(\xi_{\boldsymbol{\sigma}}, (\xi_{\mathbf{u}}^-)_t) \\ &\qquad - a_h(\eta_{\boldsymbol{\sigma}}, (\xi_{\mathbf{u}})_t) + c_h(\eta_{\boldsymbol{\sigma}}^+, (\xi_{\mathbf{u}})_t) - b_h(\xi_{\boldsymbol{\sigma}}, (\eta_{\mathbf{u}})_t) + c_h(\xi_{\boldsymbol{\sigma}}, (\eta_{\mathbf{u}}^-)_t).\end{aligned} \tag{4.15}$$

We note that the first line in the right hand side of (4.15) vanishes due to (3.2a). We then obtain

$$\begin{aligned}\frac{1}{2}\frac{d}{dt}\left(\|(\xi_{\mathbf{u}})_t\|_{L^2(\Omega)}^2 + \|\xi_{\boldsymbol{\sigma}}\|_{\mathcal{A},\Omega}^2\right) &= -((\eta_{\mathbf{u}})_{tt}, (\xi_{\mathbf{u}})_t)_\Omega - ((\mathcal{A}\eta_{\boldsymbol{\sigma}})_t, \xi_{\boldsymbol{\sigma}})_\Omega \\ &\quad - \left(-b_h(\xi_{\boldsymbol{\sigma}}, (\eta_{\mathbf{u}})_t) + c_h(\xi_{\boldsymbol{\sigma}}, (\eta_{\mathbf{u}}^-)_t)\right) + (-a_h(\eta_{\boldsymbol{\sigma}}, (\xi_{\mathbf{u}})_t) \\ &\quad + c_h(\eta_{\boldsymbol{\sigma}}^+, (\xi_{\mathbf{u}})_t)).\end{aligned} \tag{4.16}$$

We denote each term in the right hand side of (4.16) by I, II, III and IV, respectively, and we proceed to estimate them individually. For I, using (2.12), we have

$$\begin{aligned} \mathrm{I} &= -((\eta_{\mathbf{u}})_{tt}, (\xi_{\mathbf{u}})_t)_\Omega \le \|(\eta_{\mathbf{u}})_{tt}\|_{L^2(\Omega)} \|(\xi_{\mathbf{u}})_t\|_{L^2(\Omega)} \\ &\le Ch^{k+1} \|\boldsymbol{\sigma}\|_{L^\infty(0,T;H^{k+1}(\Omega))} \|(\xi_{\mathbf{u}})_t\|_{L^2(\Omega)}, \end{aligned} \tag{4.17}$$

where we have used $\|(\eta_{\mathbf{u}})_{tt}\|_{L^2(\Omega)} = \|\eta_{\mathbf{u}_{tt}}\|_{L^2(\Omega)} \le Ch^{k+1}\|\mathbf{u}_{tt}\|_{L^\infty(0,T;H^{k+1}(\Omega))} = Ch^{k+1}\|\boldsymbol{\sigma}\|_{L^\infty(0,T;H^{k+1}(\Omega))}$. For II, using (2.12) again together with the norm equivalence (3.1), we obtain

$$\begin{aligned} \mathrm{II} &= -((\mathcal{A}\eta_{\boldsymbol{\sigma}})_t, \xi_{\boldsymbol{\sigma}})_\Omega = -(\mathcal{A}\xi_{\boldsymbol{\sigma}}, (\eta_{\boldsymbol{\sigma}})_t)_\Omega \\ &\le C\sqrt{\lambda+\mu} h^{k+1} \|\boldsymbol{\sigma}\|_{W^{1,\infty}(0,T;H^{k+1}(\Omega))} \|\xi_{\boldsymbol{\sigma}}\|_{\mathcal{A},\Omega}, \end{aligned} \tag{4.18}$$

where we have used $\|(\eta_{\boldsymbol{\sigma}})_t\|_{L^2(\Omega)} = \|\eta_{\boldsymbol{\sigma}_t}\|_{L^2(\Omega)} \le Ch^{k+1}\|\boldsymbol{\sigma}\|_{W^{1,\infty}(0,T;H^{k+1}(\Omega))}$. Moreover, for III, the super-convergence property (3.4a) yields

$$\begin{aligned} \mathrm{III} &\le Ch^{k+1} \|\mathbf{u}\|_{W^{1,\infty}(0,T;H^{k+2}(\Omega))} \|\xi_{\boldsymbol{\sigma}}\|_{L^2(\Omega)} \\ &\le C\sqrt{\lambda+\mu} h^{k+1} \|\mathbf{u}\|_{W^{1,\infty}(0,T;H^{k+2}(\Omega))} \|\xi_{\boldsymbol{\sigma}}\|_{\mathcal{A},\Omega} \end{aligned} \tag{4.19}$$

where in the last inequality we have also used the norm equivalence (3.1). For IV, we apply the super-convergence property (3.4b) to obtain

$$\mathrm{IV} \le Ch^{k+1} \|\boldsymbol{\sigma}\|_{L^\infty(0,T;H^{k+2}(\Omega))} \|(\xi_{\mathbf{u}})_t\|_{L^2(\Omega)}. \tag{4.20}$$

Combining (4.17)–(4.20) with (4.16) yields

$$\begin{aligned} &\frac{1}{2}\frac{d}{dt}\left(\|(\xi_{\mathbf{u}})_t\|^2_{L^2(\Omega)} + \|\xi_{\boldsymbol{\sigma}}\|^2_{\mathcal{A},\Omega}\right) \\ &\quad \le C\sqrt{\lambda+\mu} h^{k+1} \left(\|\mathbf{u}\|_{W^{1,\infty}(0,T;H^{k+2}(\Omega))} + \|\boldsymbol{\sigma}\|_{W^{1,\infty}(0,T;H^{k+2}(\Omega))}\right) \\ &\qquad \left(\|(\xi_{\mathbf{u}})_t\|_{L^2(\Omega)} + \|\xi_{\boldsymbol{\sigma}}\|_{\mathcal{A},\Omega}\right), \end{aligned}$$

which leads to

$$\begin{aligned} &\frac{1}{2}\frac{d}{dt}\left(\|(\xi_{\mathbf{u}})_t\|^2_{L^2(\Omega)} + \|\xi_{\boldsymbol{\sigma}}\|^2_{\mathcal{A},\Omega}\right)^{1/2} \\ &\quad \le C\sqrt{\lambda+\mu} h^{k+1} \left(\|\mathbf{u}\|_{W^{1,\infty}(0,T;H^{k+2}(\Omega))} + \|\boldsymbol{\sigma}\|_{W^{1,\infty}(0,T;H^{k+2}(\Omega))}\right). \end{aligned} \tag{4.21}$$

Integrating (4.21) from 0 to t and using the estimates for the initial conditions yields

$$\left(\|(\xi_{\mathbf{u}})_t\|^2_{L^2(\Omega)} + \|\xi_{\boldsymbol{\sigma}}\|^2_{\mathcal{A},\Omega}\right)^{1/2} \le C\sqrt{\lambda+\mu}\left(\|\mathbf{u}\|_{W^{1,\infty}(0,T;H^{k+2}(\Omega))} + \|\boldsymbol{\sigma}\|_{W^{1,\infty}(0,T;H^{k+2}(\Omega))}\right) h^{k+1}(t+1). \tag{4.22}$$

Then the desired results follow from (4.22) and the estimates for $(\eta_{\mathbf{u}})_t$ and $\eta_{\boldsymbol{\sigma}}$.

□

Remark 4.2 We note that if, as a direct generation of [10], the "mixed" Gauss-Radau projection $(P_1^+ \otimes P_2, P_1 \otimes P_2^+)$ is applied to the stress tensor, the term III above should vanish; but the resulted tensor polynomial is not symmetric. To keep the symmetry, we apply the same Gauss-Radau projection to each entry of the stress tensor such that the resulted tensor polynomial is also symmetric. However since III does not vanish anymore, we need the super-convergence property (3.4a) to prove the estimate in (4.19).

In the next theorem, we show an optimal estimate for the L^2 error of the displacement $\mathbf{u}$.

Theorem 4.3 *Under the initial conditions (2.13), the following estimate holds*

$$\max_{t\in[0,T]}\|e_{\mathbf{u}}(t)\|_{L^2(\Omega)} \le Ch^{k+1}\sqrt{\lambda+\mu}(T^2+1)\left(\|\mathbf{u}\|_{W^{1,\infty}(0,T;H^{k+2}(\Omega))}+\|\boldsymbol{\sigma}\|_{W^{1,\infty}(0,T;H^{k+2}(\Omega))}\right). \tag{4.23}$$

Proof First of all, for any fixed time $t_0 \le T$, we define the following errors

$$E_{\mathbf{u}}(t)=\int_t^{t_0} e_{\mathbf{u}}(s)ds, \quad E^{\eta}_{\mathbf{u}}(t)=\int_t^{t_0}\eta_{\mathbf{u}}(s)ds, \quad E^{\xi}_{\mathbf{u}}(t)=\int_t^{t_0}\xi_{\mathbf{u}}(s)ds, \tag{4.24}$$

$$E_{\boldsymbol{\sigma}}(t)=\int_t^{t_0} e_{\boldsymbol{\sigma}}(s)ds, \quad E^{\eta}_{\boldsymbol{\sigma}}(t)=\int_t^{t_0}\eta_{\boldsymbol{\sigma}}(s)ds, \quad E^{\xi}_{\boldsymbol{\sigma}}(t)=\int_t^{t_0}\xi_{\boldsymbol{\sigma}}(s)ds. \tag{4.25}$$

We have the following estimates for these errors:

$$\|E^{\xi}_{\mathbf{u}}(t)\|_{L^2(\Omega)} \le T\|\xi_{\mathbf{u}}\|_{L^\infty(0,T;L^2(\Omega))}, \tag{4.26a}$$

$$\|E^{\eta}_{\mathbf{u}}(t)\|_{L^2(\Omega)} \le CTh^{k+1}\|\mathbf{u}\|_{L^\infty(0,T;H^{k+1}(\Omega))}, \tag{4.26b}$$

$$\|E^{\eta}_{\boldsymbol{\sigma}}(t)\|_{\mathcal{A},\Omega} \le CTh^{k+1}\|\boldsymbol{\sigma}\|_{L^\infty(0,T;H^{k+1}(\Omega))}, \tag{4.26c}$$

$$\|E^{\xi}_{\boldsymbol{\sigma}}(t)\|_{\mathcal{A},\Omega} \le C\sqrt{\lambda+\mu}T(T+1)h^{k+1}\left(\|\mathbf{u}\|_{W^{1,\infty}(0,T;H^{k+2}(\Omega))}+\|\boldsymbol{\sigma}\|_{W^{1,\infty}(0,T;H^{k+2}(\Omega))}\right), \tag{4.26d}$$

where in the last inequality we have used the estimate of $\xi_{\boldsymbol{\sigma}}$ from (4.22). Noticing that $\frac{d}{dt}E^{\xi}_{\mathbf{u}} = -\xi_{\mathbf{u}}$, we get

$$\begin{aligned}((e_{\mathbf{u}})_{tt}, E^{\xi}_{\mathbf{u}})_\Omega &= ((\xi_{\mathbf{u}})_{tt}, E^{\xi}_{\mathbf{u}})_\Omega + ((\eta_{\mathbf{u}})_{tt}, E^{\xi}_{\mathbf{u}})_\Omega \\ &= \frac{d}{dt}((\xi_{\mathbf{u}})_t, E^{\xi}_{\mathbf{u}})_\Omega + ((\xi_{\mathbf{u}})_t, \xi_{\mathbf{u}})_\Omega + ((\eta_{\mathbf{u}})_{tt}, E^{\xi}_{\mathbf{u}})_\Omega.\end{aligned}$$

Taking the test function $\mathbf{v}_h = E^{\xi}_{\mathbf{u}}(t)$ in (4.13a) and utilizing this identity, we have

$$\begin{aligned}((\xi_{\mathbf{u}})_t, \xi_{\mathbf{u}})_\Omega + a_h(\xi_{\boldsymbol{\sigma}}, E^{\xi}_{\mathbf{u}}) - c_h((\xi_{\boldsymbol{\sigma}})^+, E^{\xi}_{\mathbf{u}}) = &-\frac{d}{dt}((\xi_{\mathbf{u}})_t, E^{\xi}_{\mathbf{u}})_\Omega \\ &- ((\eta_{\mathbf{u}})_{tt}, E^{\xi}_{\mathbf{u}})_\Omega - a_h(\eta_{\boldsymbol{\sigma}}, E^{\xi}_{\mathbf{u}}) + c_h((\eta_{\boldsymbol{\sigma}})^+, E^{\xi}_{\mathbf{u}}).\end{aligned}$$

Next, integrating (4.13b), choosing $\boldsymbol{\tau}_h = \xi_{\boldsymbol{\sigma}}$, and using $E_{\boldsymbol{\sigma}} = E^{\xi}_{\boldsymbol{\sigma}} + E^{\eta}_{\boldsymbol{\sigma}}$ and $E_{\mathbf{u}} = E^{\xi}_{\mathbf{u}} + E^{\eta}_{\mathbf{u}}$, we have

$$(\mathcal{A}E^{\xi}_{\boldsymbol{\sigma}}, \xi_{\boldsymbol{\sigma}})_\Omega + b_h(\xi_{\boldsymbol{\sigma}}, E^{\xi}_{\mathbf{u}}) - c_h(\xi_{\boldsymbol{\sigma}}, (E^{\xi}_{\mathbf{u}})^-) = -(\mathcal{A}E^{\eta}_{\boldsymbol{\sigma}}, \xi_{\boldsymbol{\sigma}})_\Omega - b_h(\xi_{\boldsymbol{\sigma}}, E^{\eta}_{\mathbf{u}}) + c_h(\xi_{\boldsymbol{\sigma}}, (E^{\eta}_{\mathbf{u}})^-).$$

Now, adding the two identities above and using the identity (3.2a), we have

$$\begin{aligned}\frac{1}{2}\frac{d}{dt}(\|\xi_{\mathbf{u}}\|^2_{L^2(\Omega)} - \|E^{\xi}_{\boldsymbol{\sigma}}\|^2_{\mathcal{A},\Omega}) = &-\frac{d}{dt}((\xi_{\mathbf{u}})_t, E^{\xi}_{\mathbf{u}})_\Omega - ((\eta_{\mathbf{u}})_{tt}, E^{\xi}_{\mathbf{u}})_\Omega - a_h(\eta_{\boldsymbol{\sigma}}, E^{\xi}_{\mathbf{u}}) + c_h((\eta_{\boldsymbol{\sigma}})^+, E^{\xi}_{\mathbf{u}}) \\ &- (\mathcal{A}E^{\eta}_{\boldsymbol{\sigma}}, \xi_{\boldsymbol{\sigma}})_\Omega - b_h(\xi_{\boldsymbol{\sigma}}, E^{\eta}_{\mathbf{u}}) + c_h(\xi_{\boldsymbol{\sigma}}, (E^{\eta}_{\mathbf{u}})^-).\end{aligned} \tag{4.27}$$

Next we proceed to estimate the right hand side of (4.27), after integrating it from 0 to t_0. The super-convergence (3.4b) and (4.26a) lead to

$$\begin{aligned}\int_0^{t_0} -a_h(\eta_{\boldsymbol{\sigma}}, E^{\xi}_{\mathbf{u}}) + c_h((\eta_{\boldsymbol{\sigma}})^+, E^{\xi}_{\mathbf{u}})ds &\le \int_0^{t_0} Ch^{k+1}\|\boldsymbol{\sigma}\|_{H^{k+2}(\Omega)}\|E^{\xi}_{\mathbf{u}}\|_{L^2(\Omega)}ds \\ &\le CT^2h^{k+1}\|\boldsymbol{\sigma}\|_{L^\infty(0,T;H^{k+2}(\Omega))}\|\xi_{\mathbf{u}}\|_{L^\infty(0,T;L^2(\Omega))}.\end{aligned} \tag{4.28}$$

Similarly, using the super-convergence (3.4a) with (4.26b) and the estimate of $\xi_{\boldsymbol{\sigma}}$ from (4.22), we have

$$\begin{aligned}&\int_0^{t_0} -b_h(\xi_{\boldsymbol{\sigma}}, E_{\mathbf{u}}^{\eta}) + c_h(\xi_{\boldsymbol{\sigma}}, (E_{\mathbf{u}}^{\eta})^{-})ds \\ &\le C(\lambda+\mu)T^2(T+1)h^{2k+2}\|\mathbf{u}\|_{L^\infty(0,T;H^{k+2}(\Omega))}\left(\|\mathbf{u}\|_{W^{1,\infty}(0,T;H^{k+2}(\Omega))} + \|\boldsymbol{\sigma}\|_{W^{1,\infty}(0,T;H^{k+2}(\Omega))}\right).\end{aligned} \tag{4.29}$$

Noticing $E_{\mathbf{u}}^{\xi}(t_0) = 0$ and using the second condition in (4.7a), we obtain

$$\int_0^{t_0} -\frac{d}{dt}((\xi_{\mathbf{u}})_t, E_{\mathbf{u}}^{\xi})_{\Omega} ds = -((\xi_{\mathbf{u}})_t(t_0), E_{\mathbf{u}}^{\xi}(t_0))_{\Omega} + ((\xi_{\mathbf{u}})_t(0), E_{\mathbf{u}}^{\xi}(0))_{\Omega} = 0. \tag{4.30}$$

Besides, applying integration by parts of time over $[0, t_0]$ and the identities $\frac{d}{dt}E_{\mathbf{u}}^{\xi} = -\xi_{\mathbf{u}}$, $E_{\mathbf{u}}^{\xi}(t_0) = 0$, we get

$$\begin{aligned}\int_0^{t_0} -\big((\eta_{\mathbf{u}})_{tt}, E_{\mathbf{u}}^{\xi}\big)_{\Omega} ds &= \big(-(\eta_{\mathbf{u}})_t(t_0), E_{\mathbf{u}}^{\xi}(t_0)\big)_{\Omega} + \big((\eta_{\mathbf{u}})_t(0), E_{\mathbf{u}}^{\xi}(0)\big)_{\Omega} + \int_0^{t_0}\big((\eta_{\mathbf{u}})_t, \xi_{\mathbf{u}}\big)_{\Omega} ds \\ &= \int_0^{t_0}\big((\eta_{\mathbf{u}})_t, \xi_{\mathbf{u}}\big)_{\Omega} ds + \big((\eta_{\mathbf{u}})_t(0), E_{\mathbf{u}}^{\xi}(0)\big)_{\Omega} \\ &\le CT\|(\eta_{\mathbf{u}})_t\|_{L^\infty(0,T;L^2(\Omega))}\|\xi_{\mathbf{u}}\|_{L^\infty(0,T;L^2(\Omega))} \\ &\quad + \|(\eta_{\mathbf{u}})_t(0)\|_{L^2(\Omega)}\|E_{\mathbf{u}}^{\xi}(0)\|_{L^2(\Omega)} \\ &\le Ch^{k+1}T\|\mathbf{u}\|_{W^{1,\infty}(0,T;H^{k+1}(\Omega))}\|\xi_{\mathbf{u}}\|_{L^\infty(0,T;L^2(\Omega))},\end{aligned} \tag{4.31}$$

where in the last inequality we have also used (4.26a). Then, by (4.26c) and (4.22), we have

$$\begin{aligned}&\int_0^{t_0} -(\mathcal{A}E_{\boldsymbol{\sigma}}^{\eta}, \xi_{\boldsymbol{\sigma}})_{\Omega} ds \le \int_0^{t_0}\|E_{\boldsymbol{\sigma}}^{\eta}\|_{\mathcal{A},\Omega}\|\xi_{\boldsymbol{\sigma}}\|_{\mathcal{A},\Omega} ds \\ &\le C\sqrt{\lambda+\mu}T^2(T+1)h^{2k+2}\|\boldsymbol{\sigma}\|_{L^\infty(0,T;L^2(\Omega))}\left(\|\mathbf{u}\|_{W^{1,\infty}(0,T;H^{k+2}(\Omega))} + \|\boldsymbol{\sigma}\|_{W^{1,\infty}(0,T;H^{k+2}(\Omega))}\right).\end{aligned} \tag{4.32}$$

Now integrating (4.27) from 0 to t_0, putting (4.28)–(4.32) into the resulted equation and using (4.7a), we have

$$\begin{aligned}&\|\xi_{\mathbf{u}}(t_0)\|_{L^2(\Omega)}^2 + \|E_{\boldsymbol{\sigma}}^{\xi}(0)\|_{\mathcal{A},\Omega}^2 \\ &\le C(h^{2k+2}(\lambda+\mu)(T^2+T^3)F_1(\mathbf{u},\boldsymbol{\sigma}) + h^{k+1}(T^2+T)F_2(\mathbf{u},\boldsymbol{\sigma})\|\xi_{\mathbf{u}}\|_{L^\infty(0,T;L^2(\Omega))}),\end{aligned} \tag{4.33}$$

where $F_1(\mathbf{u},\boldsymbol{\sigma}) = \left(\|\mathbf{u}\|_{W^{1,\infty}(0,T;H^{k+2}(\Omega))} + \|\boldsymbol{\sigma}\|_{W^{1,\infty}(0,T;H^{k+2}(\Omega))}\right)^2$ and $F_2(\mathbf{u},\boldsymbol{\sigma}) = \|\mathbf{u}\|_{W^{1,\infty}(0,T;H^{k+1}(\Omega))} + \|\boldsymbol{\sigma}\|_{L^\infty(0,T;H^{k+1}(\Omega))}$. Applying Young's inequality to (4.33), we have

$$\begin{aligned}\|\xi_{\mathbf{u}}(t_0)\|_{L^2(\Omega)}^2 &\le Ch^{2k+2}(\lambda+\mu)(T^2+T^3)F_1(\mathbf{u},\boldsymbol{\sigma}) + C^2h^{2k+2}(T^2+T)^2(F_2(\mathbf{u},\boldsymbol{\sigma}))^2 \\ &\quad + \frac{1}{4}\|\xi_{\mathbf{u}}\|_{L^\infty(0,T;L^2(\Omega))}^2.\end{aligned} \tag{4.34}$$

We note that (4.34) is true for any $t_0 \in [0, T]$. So we can take t_0 to be where $\|\xi_{\mathbf{u}}\|_{L^\infty(0,T;L^2(\Omega))}$ is achieved. Then the desired result follows together with the optimal error estimate for $\eta_{\mathbf{u}}$. □

5 Fully Discrete Methods: Energy Conservation, Stability and Error Estimate

In this section, we discuss some fully discrete energy conserving schemes for the linear elastodynamics (1.1), and analyze their optimal convergence property. The spatial discretization is given by the LDG methods (2.6). Note that in (2.6b) we can always represent $\boldsymbol{\sigma}_h$ in terms of $\mathbf{u}_h$ locally on each element and put it into (2.6a) to obtain a system of ordinary differential equations for $\mathbf{u}_h$ in the form of

$$\mathbf{M}(\mathbf{U}_h)_{tt}(t) = \mathbf{A}\mathbf{U}_h(t), \tag{5.1}$$

where $\mathbf{M}$ is the mass matrix and $\mathbf{U}_h$ is the vector solution to the LDG spatial discretization (2.6). Here we shall focus on the time discretization. In the following discussion, we always let $0 = t_0 \le t_1 \le \cdots \le t_N = T$ be a partition of the entire time interval $[0, T]$ with the uniform time step $\triangle t = t_n - t_{n-1} = T/N$, $n = 1, 2, ..., N$.

5.1 A Second-order Scheme

We first consider the second-order fully-discrete leap-frog method which can inherit the property of energy conservation from the semi-discrete scheme. The leap-frog LDG method is to find a sequence of approximations $\mathbf{u}_h^n \in \mathbf{V}_h^k$ and $\boldsymbol{\sigma}_h^n \in \boldsymbol{\Sigma}_h^k$ to $\mathbf{u}^n := \mathbf{u}(t_n)$ and $\boldsymbol{\sigma}^n := \boldsymbol{\sigma}(t_n)$ satisfying the equations

$$\left(\frac{\mathbf{u}_h^{n+1} - 2\mathbf{u}_h^n + \mathbf{u}_h^{n-1}}{\triangle t^2}, \mathbf{v}_h\right)_\Omega + a_h(\boldsymbol{\sigma}_h^n, \mathbf{v}_h) - c_h((\boldsymbol{\sigma}_h^n)^+, \mathbf{v}_h) = 0, \qquad \forall \mathbf{v}_h \in \mathbf{V}_h^k, \tag{5.2a}$$

$$(\mathcal{A}\boldsymbol{\sigma}_h^n, \boldsymbol{\tau}_h)_\Omega + b_h(\boldsymbol{\tau}_h, \mathbf{u}_h^n) - c_h(\boldsymbol{\tau}_h, (\mathbf{u}_h^n)^-) = 0, \qquad \forall \boldsymbol{\tau}_h \in \boldsymbol{\Sigma}_h^k, \tag{5.2b}$$

together with two initial conditions

$$\mathbf{u}_h^0 = \mathbf{P}^-\mathbf{u}_0, \quad \text{and} \quad \mathbf{u}_h^1 = \mathbf{P}^-\mathbf{u}_0 + \triangle t\mathbf{P}^-\mathbf{v}_0 + \frac{\triangle t^2}{2}\mathbf{P}^-\mathbf{u}_{tt}(0), \tag{5.2c}$$

where $\mathbf{u}_{tt}(0)$ can be computed by $\nabla \cdot \boldsymbol{\sigma}(\mathbf{u}_0)$. Note that the choice of $\mathbf{u}_h^1$ involves the first three terms of the related Taylor expansion. For higher-order temporal discretization, more terms should be involved in the initial condition, see the discussion in Sect. 5.2. Next, we begin with presenting the exact conservation of a discrete energy which approximates the continuous energy $E(t)$ in (2.16).

Theorem 5.1 *For the leap-frog LDG method (5.2), the following energy conserves for all integers $n \ge 0$*

$$E_h^{n+1} = \frac{1}{2\Delta t^2}\|\mathbf{u}_h^{n+1} - \mathbf{u}_h^n\|^2_{L^2(\Omega)} + G_h^{n+1}, \quad \textit{where} \quad G_h^{n+1} := \frac{1}{2}(\mathcal{A}\boldsymbol{\sigma}_h^{n+1}, \boldsymbol{\sigma}_h^n)_\Omega \\ \frac{1}{2}(\mathcal{A}\boldsymbol{\sigma}_h^n, \boldsymbol{\sigma}_h^{n+1})_\Omega. \tag{5.3}$$

Proof In (5.2a), we take $\mathbf{v}_h = \left(\mathbf{u}_h^{n+1} - \mathbf{u}_h^{n-1}\right)/(2\Delta t)$ and obtain

$$\left(\frac{\mathbf{u}_h^{n+1} - 2\mathbf{u}_h^n + \mathbf{u}_h^{n-1}}{\triangle t^2}, \frac{\mathbf{u}_h^{n+1} - \mathbf{u}_h^{n-1}}{2\Delta t}\right)_\Omega + a_h\left(\boldsymbol{\sigma}_h^n, \frac{\mathbf{u}_h^{n+1} - \mathbf{u}_h^{n-1}}{2\Delta t}\right)$$

$$-c_h\left((\boldsymbol{\sigma}_h^n)^+, \frac{\mathbf{u}_h^{n+1}-\mathbf{u}_h^{n-1}}{2\Delta t}\right)=0. \tag{5.4}$$

Then, we take the difference of (5.2b) at time step t_{n+1} and t_{n-1}, and choose $\boldsymbol{\tau}_h=\boldsymbol{\sigma}_h^n/(2\Delta t)$, which leads to

$$\left(\frac{\mathcal{A}\boldsymbol{\sigma}_h^{n+1}-\mathcal{A}\boldsymbol{\sigma}_h^{n-1}}{2\Delta t}, \boldsymbol{\sigma}_h^n\right)_\Omega + b_h\left(\boldsymbol{\sigma}_h^n, \frac{\mathbf{u}_h^{n+1}-\mathbf{u}_h^{n-1}}{2\Delta t}\right) - c_h\left(\boldsymbol{\sigma}_h^n, \frac{(\mathbf{u}_h^{n+1})^- - (\mathbf{u}_h^{n-1})^-}{2\Delta t}\right)=0. \tag{5.5}$$

Now we note that $(\mathbf{u}_h^{n+1}-2\mathbf{u}_h^n+\mathbf{u}_h^{n-1}, \mathbf{u}_h^{n+1}-\mathbf{u}_h^{n-1})_\Omega = \|\mathbf{u}_h^{n+1}-\mathbf{u}_h^n\|^2_{L^2(\Omega)} - \|\mathbf{u}_h^n-\mathbf{u}_h^{n-1}\|^2_{L^2(\Omega)}$. By the definition of G_h^n in (5.3), the sum of the Eqs. (5.4) and (5.5) yields

$$\begin{aligned}\frac{1}{\Delta t}\left(E_h^{n+1}-E_h^n\right) &= \frac{1}{\Delta t}\left(\frac{\|\mathbf{u}_h^{n+1}-\mathbf{u}_h^n\|^2_{L^2(\Omega)}}{2\Delta t^2}+G_h^{n+1}-\frac{\|\mathbf{u}_h^n-\mathbf{u}_h^{n-1}\|^2_{L^2(\Omega)}}{2\Delta t^2}-G_h^n\right)\\ &= -\frac{1}{2\Delta t}\Big(a_h(\boldsymbol{\sigma}_h^n, \mathbf{u}_h^{n+1}-\mathbf{u}_h^{n-1}) + b_h(\boldsymbol{\sigma}_h^n, \mathbf{u}_h^{n+1}-\mathbf{u}_h^{n-1})\\ &\quad -c_h((\boldsymbol{\sigma}_h^n)^+, \mathbf{u}_h^{n+1}-\mathbf{u}_h^{n-1}) - c_h(\boldsymbol{\sigma}_h^n, (\mathbf{u}_h^{n+1})^- - (\mathbf{u}_h^{n-1})^-)\Big)\\ &= 0,\end{aligned}$$

where the last equality holds due to the identity (3.2a). Therefore, the energy conservation property (5.3) follows. □

In order to analyze the stability and solution errors of the fully discrete LDG scheme (5.2), we need the following trace and inverse inequalities [53]

$$\|p\|_{L^2(\partial K)} \le C_t\sqrt{(k+1)(k+2)}h^{-1/2}\|p\|_{L^2(T)}, \qquad \forall p\in\mathbb{Q}^k(T), \tag{5.6a}$$

$$\|\nabla p\|_{L^2(T)} \le C_i(2+\sqrt{k(k+1)})h^{-1}\|p\|_{L^2(T)}, \qquad \forall p\in\mathbb{Q}^k(T), \tag{5.6b}$$

where the constants C_t and C_i only depend on the mesh regularity. Then we can prove the following CFL condition for the stability of the fully discrete LDG scheme (5.2).

Theorem 5.2 *The leap-frog LDG scheme (5.2) is stable if the CFL condition*

$$\triangle t < \frac{C_S h}{(2+\sqrt{k(k+1)}+(k+1)(k+2))\sqrt{\lambda+\mu}} \tag{5.7}$$

is satisfied for some constant C_S only depending on the mesh regularity.

Proof In (5.2a), we take $\mathbf{v}_h=\mathbf{u}_h^{n+1}-\mathbf{u}_h^{n-1}$ and obtain

$$\frac{\|\mathbf{u}_h^{n+1}-\mathbf{u}_h^n\|_{L^2(\Omega)}}{\triangle t^2} - \frac{\|\mathbf{u}_h^n-\mathbf{u}_h^{n-1}\|_{L^2(\Omega)}}{\triangle t^2} + a_h(\boldsymbol{\sigma}_h^n, \mathbf{u}_h^{n+1}-\mathbf{u}_h^{n-1}) - c_h((\boldsymbol{\sigma}_h^n)^+, \mathbf{u}_h^{n+1}-\mathbf{u}_h^{n-1})=0. \tag{5.8}$$

In addition, we take the difference of (5.2b) at time step t_n and t_{n+1}, and choose $\boldsymbol{\tau}_h = \boldsymbol{\sigma}_h^{n+1}+\boldsymbol{\sigma}_h^n$ to obtain

$$\begin{aligned}&(\mathcal{A}\boldsymbol{\sigma}_h^{n+1}-\mathcal{A}\boldsymbol{\sigma}_h^n, \boldsymbol{\sigma}_h^{n+1}+\boldsymbol{\sigma}_h^n)_\Omega + b_h(\boldsymbol{\sigma}_h^{n+1}+\boldsymbol{\sigma}_h^n, \mathbf{u}_h^{n+1}\\ &\quad -\mathbf{u}_h^n) - c_h(\boldsymbol{\sigma}_h^{n+1}+\boldsymbol{\sigma}_h^n, (\mathbf{u}_h^{n+1})^- - (\mathbf{u}_h^n)^-)=0.\end{aligned} \tag{5.9}$$

Using the identity (3.2a), we have

$$\begin{aligned} &a_h(\boldsymbol{\sigma}_h^n, \mathbf{u}_h^{n+1} - \mathbf{u}_h^{n-1}) - c_h((\boldsymbol{\sigma}_h^n)^+, \mathbf{u}_h^{n+1} - \mathbf{u}_h^{n-1}) \\ &\quad = -b_h(\boldsymbol{\sigma}_h^n, \mathbf{u}_h^{n+1} - \mathbf{u}_h^{n-1}) + c_h(\boldsymbol{\sigma}_h^n, (\mathbf{u}_h^{n+1})^- - (\mathbf{u}_h^{n-1})^-). \end{aligned} \tag{5.10}$$

Putting (5.10) into (5.8) and adding it to (5.9), we obtain

$$\begin{aligned} &\frac{\|\mathbf{u}_h^{n+1} - \mathbf{u}_h^n\|^2_{L^2(\Omega)}}{\triangle t^2} - \frac{\|\mathbf{u}_h^n - \mathbf{u}_h^{n-1}\|^2_{L^2(\Omega)}}{\triangle t^2} + (\mathcal{A}\boldsymbol{\sigma}_h^{n+1}, \boldsymbol{\sigma}_h^{n+1})_{L^2(\Omega)} - (\mathcal{A}\boldsymbol{\sigma}_h^n, \boldsymbol{\sigma}_h^n)_{L^2(\Omega)} \\ &+b_h(\boldsymbol{\sigma}_h^{n+1}, \mathbf{u}_h^{n+1} - \mathbf{u}_h^n) - b_h(\boldsymbol{\sigma}_h^n, \mathbf{u}_h^n - \mathbf{u}_h^{n-1}) + c_h(\boldsymbol{\sigma}_h^{n+1}, (\mathbf{u}_h^{n+1})^- - (\mathbf{u}_h^n)^-) \\ &-c_h(\boldsymbol{\sigma}_h^n, (\mathbf{u}_h^n)^- - (\mathbf{u}_h^{n-1})^-) = 0. \end{aligned} \tag{5.11}$$

Now summing (5.11) from 1 to any integer $M \le N$, we arrive at

$$\begin{aligned} &\frac{\|\mathbf{u}_h^{M+1} - \mathbf{u}_h^M\|^2_{L^2(\Omega)}}{\triangle t^2} + (\mathcal{A}\boldsymbol{\sigma}_h^{M+1}, \boldsymbol{\sigma}_h^{M+1})_{L^2(\Omega)} - \frac{\|\mathbf{u}_h^1 - \mathbf{u}_h^0\|^2_{L^2(\Omega)}}{\triangle t^2} - (\mathcal{A}\boldsymbol{\sigma}_h^1, \boldsymbol{\sigma}_h^1)_{L^2(\Omega)} \\ &+b_h(\boldsymbol{\sigma}_h^{M+1}, \mathbf{u}_h^{M+1} - \mathbf{u}_h^M) + c_h(\boldsymbol{\sigma}_h^{M+1}, (\mathbf{u}_h^{M+1})^- - (\mathbf{u}_h^M)^-) \\ &-b_h(\boldsymbol{\sigma}_h^1, \mathbf{u}_h^1 - \mathbf{u}_h^0) - c(\boldsymbol{\sigma}_h^1, (\mathbf{u}_h^1)^- - (\mathbf{u}_h^0)^-) = 0. \end{aligned} \tag{5.12}$$

Then by Hölder's inequality with the inverse and trace inequalities in (5.6), we have

$$b_h(\boldsymbol{\sigma}_h^{M+1}, \mathbf{u}_h^{M+1} - \mathbf{u}_h^M) \le C_i(2 + \sqrt{k(k+1)})h^{-1}\|\boldsymbol{\sigma}_h^{M+1}\|_{L^2(\Omega)}\|\mathbf{u}_h^{M+1} - \mathbf{u}_h^M\|_{L^2(\Omega)}, \tag{5.13}$$

$$c_h(\boldsymbol{\sigma}_h^{M+1}, (\mathbf{u}_h^{M+1})^- - (\mathbf{u}_h^M)^-) \le C_t^2(k+1)(k+2)h^{-1}\|\boldsymbol{\sigma}_h^{M+1}\|_{L^2(\Omega)}\|\mathbf{u}_h^{M+1} - \mathbf{u}_h^M\|_{L^2(\Omega)}. \tag{5.14}$$

Therefore, by Young's inequality together with the norm equivalence (3.1), we have

$$\begin{aligned} &|b_h(\boldsymbol{\sigma}_h^{M+1}, \mathbf{u}_h^{M+1} - \mathbf{u}_h^M) + c_h(\boldsymbol{\sigma}_h^{M+1}, (\mathbf{u}_h^{M+1})^- - (\mathbf{u}_h^M)^-)| \\ &\le \frac{(C_i + C_t^2)^2(2 + \sqrt{k(k+1)} + (k+1)(k+2))^2\triangle t^2 2(\lambda + \mu)}{2h^2}\|\boldsymbol{\sigma}_h^{M+1}\|^2_{\mathcal{A},\Omega} \\ &\quad + \frac{1}{2}\frac{\|\mathbf{u}_h^{M+1} - \mathbf{u}_h^M\|^2_{L^2(\Omega)}}{\triangle t^2}. \end{aligned} \tag{5.15}$$

Putting (5.15) into (5.12) yields

$$\begin{aligned} &\frac{1}{2}\frac{\|\mathbf{u}_h^{M+1} - \mathbf{u}_h^M\|^2_{L^2(\Omega)}}{\triangle t^2} + \left(1 - \frac{(C_i + C_t^2)^2(2 + \sqrt{k(k+1)} + (k+1)(k+2))^2\triangle t^2(\lambda + \mu)}{h^2}\right) \\ &\|\boldsymbol{\sigma}_h^{M+1}\|^2_{\mathcal{A},\Omega} \le \frac{\|\mathbf{u}_h^1 - \mathbf{u}_h^0\|_{L^2(\Omega)}}{\triangle t^2} + \|\boldsymbol{\sigma}_h^1\|_{\mathcal{A},\Omega} + b_h(\boldsymbol{\sigma}_h^1, \mathbf{u}_h^1 - \mathbf{u}_h^0) + c_h(\boldsymbol{\sigma}_h^1, (\mathbf{u}_h^1)^- - (\mathbf{u}_h^0)^-). \end{aligned} \tag{5.16}$$

Let

$$\frac{(C_i + C_t^2)^2(2 + \sqrt{k(k+1)} + (k+1)(k+2))^2\triangle t^2(\lambda + \mu)}{h^2} \le 1 - \varepsilon \tag{5.17}$$

with ε being a positive number. Without loss of generality, we can let $\epsilon = 1/2$ and thus finish the proof. □

We note that the dependence of the constant in (5.7) on the polynomial degree k is $(2+\sqrt{k(k+1)}+(k+1)(k+2)) \approx O(k^2)$. The numerical results in Sect. 6 indicate that this detailed formula of both k and λ, μ is sharp. Next, we proceed to estimate the fully discrete solution errors. For this purpose, without causing confusion, we denote δ_{tt} as both the discrete and continuous second-order temporal differential operator

$$\delta_{tt}\mathbf{u}_h^n = \frac{\mathbf{u}_h^{n+1} - 2\mathbf{u}_h^n + \mathbf{u}_h^{n-1}}{2\triangle t} \quad \text{and} \quad \delta_{tt}\mathbf{u}^n = \mathbf{u}_{tt}(t_n), \tag{5.18}$$

and denote δ_t as the first-order temporal differential operator

$$\delta_t \xi_{\mathbf{u}}^n := \frac{\xi_{\mathbf{u}}^n - \xi_{\mathbf{u}}^{n-1}}{\triangle t} \quad \text{and} \quad \delta_t \eta_{\mathbf{u}}^n := \frac{\eta_{\mathbf{u}}^n - \eta_{\mathbf{u}}^{n-1}}{\triangle t}.$$

In particular, we have $\delta_t \xi_{\mathbf{u}}^1 = \frac{1}{\triangle t}(\mathbf{P}^-\mathbf{u}^1 - \mathbf{u}_h^1)$ and $\delta_t \eta_{\mathbf{u}}^1 = \frac{1}{\triangle t}((\mathbf{u}^1 - \mathbf{u}^0) - \mathbf{P}^-(\mathbf{u}^1 - \mathbf{u}^0))$. Similar to (4.6), we introduce the following decomposition at discrete time steps

$$e_{\mathbf{u}}^n = \mathbf{u}^n - \mathbf{u}_h^n = \xi_{\mathbf{u}}^n + \eta_{\mathbf{u}}^n, \quad \text{where } \eta_{\mathbf{u}}^n = \mathbf{u}^n - \mathbf{P}^-\mathbf{u}^n, \quad \xi_{\mathbf{u}}^n = \mathbf{P}^-\mathbf{u}^n - \mathbf{u}_h^n, \tag{5.19a}$$

$$e_{\boldsymbol{\sigma}}^n = \boldsymbol{\sigma}^n - \boldsymbol{\sigma}_h^n = \xi_{\boldsymbol{\sigma}}^n + \eta_{\boldsymbol{\sigma}}^n, \quad \text{where } \eta_{\boldsymbol{\sigma}}^n = \boldsymbol{\sigma}^n - \boldsymbol{\Pi}^+\boldsymbol{\sigma}^n, \quad \xi_{\boldsymbol{\sigma}}^n = \boldsymbol{\Pi}^+\boldsymbol{\sigma}^n - \boldsymbol{\sigma}_h^n. \tag{5.19b}$$

In addition, we introduce a discrete energy error:

$$\mathcal{E}_h^n = \|\delta_t \xi_{\mathbf{u}}^n\|_{L^2(\Omega)} + \|\xi_{\boldsymbol{\sigma}}^n\|_{\mathcal{A},\Omega}. \tag{5.20}$$

Next, we show a group of estimates for the initial conditions (5.2c).

Lemma 5.1 *Under the initial conditions (5.2c), the following estimates hold*

$$\|\delta_t \xi_{\mathbf{u}}^1\|_{L^2(\Omega)} \le C\triangle t^2 \|\boldsymbol{\sigma}\|_{W^{1,\infty}(0,T;L^2(\Omega))}, \tag{5.21a}$$

$$\|\delta_t \eta_{\mathbf{u}}^1\|_{L^2(\Omega)} \le Ch^{k+1} \|\mathbf{u}\|_{W^{1,\infty}(0,T;H^{k+1}(\Omega))}, \tag{5.21b}$$

$$\|\xi_{\boldsymbol{\sigma}}^1\|_{\mathcal{A},\Omega} \le C\sqrt{\lambda+\mu}(h^{k+1}\|\mathbf{u}\|_{L^\infty(0,T;H^{k+2}(\Omega))} + (\triangle t^3 h^{-1} + h^{k+1})\|\boldsymbol{\sigma}\|_{W^{1,\infty}(0,T;H^{k+1}(\Omega))}), \tag{5.21c}$$

$$\|\eta_{\boldsymbol{\sigma}}^1\|_{\mathcal{A},\Omega} \le Ch^{k+1}\|\boldsymbol{\sigma}\|_{L^\infty(0,T;H^{k+1}(\Omega))}. \tag{5.21d}$$

Proof For (5.21b), by Taylor expansions, there exists some $\theta_1 \in (0, \triangle t)$ such that $\mathbf{u}^1 = \mathbf{u}(\triangle t) = \mathbf{u}^0 + \triangle t\mathbf{u}_t(\theta_1)$. Then, the estimate (2.12) leads to

$$\|\delta_t \eta_{\mathbf{u}}^1\|_{L^2(\Omega)} = \|\mathbf{u}_t(\theta_1) - \mathbf{P}^-\mathbf{u}_t(\theta_1)\|_{L^2(\Omega)} \le Ch^{k+1}\|\mathbf{u}\|_{W^{1,\infty}(0,T;H^{k+1}(\Omega))}. \tag{5.22}$$

For (5.21a), also by Taylor expansions, there exists some $\theta_2 \in (0, \triangle t)$ such that

$$\mathbf{u}^1 = \mathbf{u}(\triangle t) = \mathbf{u}^0 + \triangle t\mathbf{u}_t(0) + \frac{\triangle t^2}{2}\mathbf{u}_{tt}(0) + \frac{\triangle t^3}{6}\mathbf{u}_{ttt}(\theta_2). \tag{5.23}$$

Then, the boundedness of $\mathbf{P}^-$ yields

$$\|\delta_t \xi_{\mathbf{u}}^1\|_{L^2(\Omega)} = \frac{\triangle t^2}{6}\|\mathbf{P}^-\mathbf{u}_{ttt}(\theta_2)\|_{L^2(\Omega)} \le C\frac{\triangle t^2}{6}\|\mathbf{u}_{ttt}(\theta_2)\|_{L^2(\Omega)} \le C\triangle t^2\|\boldsymbol{\sigma}\|_{W^{1,\infty}(0,T;L^2(\Omega))}. \tag{5.24}$$

In addition, we note that (5.21d) directly follows from the estimate (2.12).

For (5.21c), by the Taylor expansion (5.23) and the estimate similar to (5.24) together with the trace and inverse inequality, we have

$$b_h(\boldsymbol{\tau}_h, \mathbf{P}^-\mathbf{u}^1 - \mathbf{u}_h^1) \le Ch^{-1}\|\boldsymbol{\tau}_h\|_{L^2(\Omega)}\|\mathbf{P}^-\mathbf{u}^1 - \mathbf{u}_h^1\|_{L^2(\Omega)}$$

$$\leq Ch^{-1}\triangle t^3\|\boldsymbol{\tau}_h\|_{L^2(\Omega)}\|\boldsymbol{\sigma}\|_{W^{1,\infty}(0,T;L^2(\Omega))}. \tag{5.25}$$

$$c_h(\boldsymbol{\tau}_h,(\mathbf{P}^-\mathbf{u}^1-\mathbf{u}_h^1)^-))\leq Ch^{-1}\|\boldsymbol{\tau}_h\|_{L^2(\Omega)}\|\mathbf{P}^-\mathbf{u}^1-\mathbf{u}_h^1\|_{L^2(\Omega)}$$
$$\leq Ch^{-1}\triangle t^3\|\boldsymbol{\tau}_h\|_{L^2(\Omega)}\|\boldsymbol{\sigma}\|_{W^{1,\infty}(0,T;L^2(\Omega))}. \tag{5.26}$$

Putting (5.25) and (5.26) together, we obtain

$$|b_h(\boldsymbol{\tau}_h,\mathbf{P}^-\mathbf{u}^1-\mathbf{u}_h^1)-c_h(\boldsymbol{\tau}_h,(\mathbf{P}^-\mathbf{u}^1-\mathbf{u}_h^1)^-)|\leq Ch^{-1}\triangle t^3\|\boldsymbol{\tau}_h\|_{L^2(\Omega)}\|\boldsymbol{\sigma}\|_{W^{1,\infty}(0,T;L^2(\Omega))}. \tag{5.27}$$

Besides, by the super-convergence property (3.4a), we have

$$|b_h(\boldsymbol{\tau}_h,\mathbf{P}^-\mathbf{u}^1-\mathbf{u}^1)-c_h(\boldsymbol{\tau}_h,(\mathbf{P}^-\mathbf{u}^1-\mathbf{u}^1)^-)|\leq Ch^{k+1}\|\boldsymbol{\tau}_h\|_{L^2(\Omega)}\|\mathbf{u}\|_{L^\infty(0,T;H^{k+2}(\Omega))}. \tag{5.28}$$

Combining (5.27) and (5.28), we arrive at

$$\begin{aligned}(\mathcal{A}(\boldsymbol{\sigma}^1-\boldsymbol{\sigma}_h^1),\boldsymbol{\tau}_h)_\Omega &= b(\boldsymbol{\tau}_h,\mathbf{u}^1-\mathbf{u}_h^1)-c(\boldsymbol{\tau}_h,(\mathbf{u}^1-\mathbf{u}_h^1)^-)\\ &\leq C(h^{k+1}\|\mathbf{u}\|_{L^\infty(0,T;H^{k+2}(\Omega))}+h^{-1}\triangle t^3\|\boldsymbol{\sigma}\|_{W^{1,\infty}(0,T;L^2(\Omega))})\|\boldsymbol{\tau}_h\|_{L^2(\Omega)}.\end{aligned} \tag{5.29}$$

Applying the similar argument to derive (4.10) from (4.9), we can obtain (5.21c) from (5.21d) and (5.29). □

We also need the following estimate for the discrete temporal derivative of projection errors.

Lemma 5.2 *There holds*

$$\|\delta_{tt}\eta_{\mathbf{u}}^n\|_{L^2(\Omega)}\leq Ch^{k+1}\|\mathbf{u}\|_{W^{2,\infty}(0,T;H^{k+1}(\Omega))}+C\triangle t^2\|\boldsymbol{\sigma}\|_{W^{2,\infty}(0,T;L^2(\Omega))}. \tag{5.30}$$

Proof By Taylor's expansion, there exist $\theta_1\in(t_n,t_{n+1})$ and $\theta_2\in(t_{n-1},t_n)$ such that

$$\mathbf{u}^{n+1}=\mathbf{u}(t_{n+1})=\mathbf{u}(t_n)+\triangle t\mathbf{u}_t(t_n)+\frac{\triangle t^2}{2}\mathbf{u}_{tt}(t_n)+\frac{\triangle t^3}{6}\mathbf{u}_{ttt}(t_n)+\frac{\triangle t^4}{24}\mathbf{u}_{tttt}(\theta_1), \tag{5.31}$$

$$\mathbf{u}^{n-1}=\mathbf{u}(t_{n-1})=\mathbf{u}(t_n)-\triangle t\mathbf{u}_t(t_n)+\frac{\triangle t^2}{2}\mathbf{u}_{tt}(t_n)-\frac{\triangle t^3}{6}\mathbf{u}_{ttt}(t_n)+\frac{\triangle t^4}{24}\mathbf{u}_{tttt}(\theta_2). \tag{5.32}$$

Then we have

$$\delta_{tt}\mathbf{P}^-\mathbf{u}^n=\frac{\mathbf{P}^-\mathbf{u}^{n+1}-2\mathbf{P}^-\mathbf{u}^n+\mathbf{P}^-\mathbf{u}^{n-1}}{\triangle t^2}=\mathbf{P}^-\mathbf{u}_{tt}^n+\frac{\triangle t^2}{24}(\mathbf{P}^-\mathbf{u}_{tttt}(\theta_1)+\mathbf{P}^-\mathbf{u}_{tttt}(\theta_2)). \tag{5.33}$$

Therefore, applying the optimal approximation and boundedness of the projection operator $\mathbf{P}^-$, we finally get

$$\begin{aligned}\|\delta_{tt}\eta_{\mathbf{u}}^n\|_{L^2(\Omega)}&=\|\delta_{tt}\mathbf{P}^-\mathbf{u}^n-\mathbf{u}_{tt}^n\|_{L^2(\Omega)}\\ &\leq\|\mathbf{P}^-\mathbf{u}_{tt}^n-\mathbf{u}_{tt}^n\|_{L^2(\Omega)}+\frac{\triangle t^2}{24}\|\mathbf{P}^-\mathbf{u}_{tttt}(\theta_1)+\mathbf{P}^-\mathbf{u}_{tttt}(\theta_2)\|_{L^2(\Omega)}\\ &\leq Ch^{k+1}\|\mathbf{u}_{tt}(t_n)\|_{H^{k+1}(\Omega)}+\frac{\triangle t^2}{24}(\|\boldsymbol{\sigma}_{tt}(\theta_1)\|_{L^2(\Omega)}+\|\boldsymbol{\sigma}_{tt}(\theta_2)\|_{L^2(\Omega)})\end{aligned} \tag{5.34}$$

which finishes the proof. □

We then present the super-convergence results involving two adjacent time steps.

Lemma 5.3 *For any* $\mathbf{v}_h \in \mathbf{V}_h^k$ *and* $\boldsymbol{\tau}_h \in \boldsymbol{\Sigma}_h^k$, *there holds*

$$\begin{aligned}
&|b_h(\boldsymbol{\tau}_h, \eta_{\mathbf{u}}^{n+1} - \eta_{\mathbf{u}}^n) - c_h(\boldsymbol{\tau}_h, (\eta_{\mathbf{u}}^{n+1})^- - (\eta_{\mathbf{u}}^n)^-) \\
&\le C\triangle t h^{k+1} \|\mathbf{u}\|_{W^{1,\infty}(0,T;H^{k+2}(\Omega))} \|\boldsymbol{\tau}_h\|_{L^2(\Omega)}, \qquad (5.35a) \\
&|a_h(\eta_{\boldsymbol{\sigma}}^{n+1} - \eta_{\boldsymbol{\sigma}}^n, \mathbf{v}_h) - c_h((\eta_{\boldsymbol{\sigma}}^{n+1})^+ - (\eta_{\boldsymbol{\sigma}}^n)^+, \mathbf{v}_h) \\
&\le C\triangle t h^{k+1} \|\boldsymbol{\sigma}\|_{W^{1,\infty}(0,T;H^{k+2}(\Omega))} \|\mathbf{v}_h\|_{L^2(\Omega)}. \qquad (5.35b)
\end{aligned}$$

Proof Without loss of generality, we only need to prove (5.35a). Again, by the Taylor's expansion, there exists $\theta \in (t_n, t_{n+1})$ such that $\mathbf{u}^{n+1} = \mathbf{u}^n + \triangle t \mathbf{u}_t(\theta)$. Then, we can write $\eta_{\mathbf{u}}^{n+1} - \eta_{\mathbf{u}}^n = (\mathbf{u}^{n+1} - \mathbf{u}^n) - \mathbf{P}^-(\mathbf{u}^{n+1} - \mathbf{u}^n) = \triangle t(\mathbf{u}_t(\theta) - \mathbf{P}^-\mathbf{u}_t(\theta))$. Therefore, using (3.4a), we obtain

$$\begin{aligned}
&|b_h(\boldsymbol{\tau}_h, \eta_{\mathbf{u}}^{n+1} - \eta_{\mathbf{u}}^n) - c_h(\boldsymbol{\tau}_h, (\eta_{\mathbf{u}}^{n+1})^- - (\eta_{\mathbf{u}}^n)^-)| \\
&\quad = \triangle t |b_h(\boldsymbol{\tau}_h, \mathbf{u}_t(\theta) - \mathbf{P}^-\mathbf{u}_t(\theta)) - c_h(\boldsymbol{\tau}_h, (\mathbf{u}_t(\theta) - \mathbf{P}^-\mathbf{u}_t(\theta))^-)| \qquad (5.36) \\
&\quad \le C\triangle t h^{k+1} \|\mathbf{u}_t(\theta)\|_{H^{k+2}(\Omega)} \|\boldsymbol{\tau}_h\|_{L^2(\Omega)}
\end{aligned}$$

which finishes the proof. □

Similarly, we have the following estimate on the difference of the inner product at two adjacent time steps.

Lemma 5.4 *For any* $\mathbf{v}_h \in \mathbf{V}_h^k$ *and* $\boldsymbol{\tau}_h \in \boldsymbol{\Sigma}_h^k$, *there holds*

$$\begin{aligned}
&|(\eta_{\mathbf{u}}^{n+1} - \eta_{\mathbf{u}}^n, \mathbf{v}_h)_\Omega| \le C\triangle t h^{k+1} \|\mathbf{u}\|_{W^{1,\infty}(0,T;H^{k+1}(\Omega))} \|\mathbf{v}_h\|_{L^2(\Omega)}, \qquad (5.37a) \\
&|(\eta_{\boldsymbol{\sigma}}^{n+1} - \eta_{\boldsymbol{\sigma}}^n, \boldsymbol{\tau}_h)_{\mathcal{A},\Omega}| \le C\triangle t h^{k+1} \|\boldsymbol{\sigma}\|_{W^{1,\infty}(0,T;H^{k+1}(\Omega))} \|\boldsymbol{\tau}_h\|_{\mathcal{A},\Omega}. \qquad (5.37b)
\end{aligned}$$

With all these preparations, now we are ready to show the following optimal error estimate for the discrete energy error defined in (5.20).

Lemma 5.5 *Given* $\triangle t$ *small enough such that* (5.7) *is satisfied, then for every integer* $1 \le n \le N$ *there holds*

$$\begin{aligned}
(\mathcal{E}_h^n)^2 \le\ & C^*\sqrt{\lambda+\mu}\triangle t(\triangle t^2 + h^{k+1}) \left(\|\mathbf{u}\|_{W^{2,\infty}(0,T;H^{k+2}(\Omega))} + \|\boldsymbol{\sigma}\|_{W^{2,\infty}(0,T;H^{k+2}(\Omega))}\right) \sum_{i=1}^n \mathcal{E}_h^i \\
&+ (C^*)^2(\lambda+\mu)(\triangle t^2 + h^{k+1})^2 (\|\mathbf{u}\|_{W^{2,\infty}(0,T;H^{k+2}(\Omega))} + \|\boldsymbol{\sigma}\|_{W^{2,\infty}(0,T;H^{k+2}(\Omega))})^2. \qquad (5.38)
\end{aligned}$$

Proof First of all, by subtracting (5.2a) from the equation for the exact solution, using the decomposition (5.19) and taking $\mathbf{v}_h = \xi_{\mathbf{u}}^{n+1} - \xi_{\mathbf{u}}^{n-1}$, we obtain the identity

$$\begin{aligned}
&\frac{\|\xi_{\mathbf{u}}^{n+1} - \xi_{\mathbf{u}}^n\|_{L^2(\Omega)}^2}{\triangle t^2} - \frac{\|\xi_{\mathbf{u}}^n - \xi_{\mathbf{u}}^{n-1}\|_{L^2(\Omega)}^2}{\triangle t^2} + a_h(\xi_{\boldsymbol{\sigma}}^n, \xi_{\mathbf{u}}^{n+1} - \xi_{\mathbf{u}}^{n-1}) - c_h((\xi_{\boldsymbol{\sigma}}^n)^+, \xi_{\mathbf{u}}^{n+1} - \xi_{\mathbf{u}}^{n-1}) \\
&= -(\delta_{tt}\eta_{\mathbf{u}}^n, \xi_{\mathbf{u}}^{n+1} - \xi_{\mathbf{u}}^{n-1})_\Omega - a_h(\eta_{\boldsymbol{\sigma}}^n, \xi_{\mathbf{u}}^{n+1} - \xi_{\mathbf{u}}^{n-1}) + c_h((\eta_{\boldsymbol{\sigma}}^n)^+, \xi_{\mathbf{u}}^{n+1} - \xi_{\mathbf{u}}^{n-1}). \qquad (5.39)
\end{aligned}$$

Similarly, by subtracting (5.2b) from the equation for the exact solutions at t_{n+1} and t_n, using the decomposition (5.19), applying $\boldsymbol{\tau}_h = \xi_{\boldsymbol{\sigma}}^{n+1} + \xi_{\boldsymbol{\sigma}}^n$ and taking the difference of the resulted two equations, we have

$$\begin{aligned}&\|\xi_{\boldsymbol{\sigma}}^{n+1}\|_{\mathcal{A},\Omega}^2-\|\xi_{\boldsymbol{\sigma}}^{n}\|_{\mathcal{A},\Omega}^2+b_h(\xi_{\boldsymbol{\sigma}}^{n+1}+\xi_{\boldsymbol{\sigma}}^{n},\xi_{\mathbf{u}}^{n+1}-\xi_{\mathbf{u}}^{n})-c_h(\xi_{\boldsymbol{\sigma}}^{n+1}+\xi_{\boldsymbol{\sigma}}^{n},(\xi_{\mathbf{u}}^{n+1})^{-}-(\xi_{\mathbf{u}}^{n})^{-})\\&\quad=-(\mathcal{A}\eta_{\boldsymbol{\sigma}}^{n+1}-\mathcal{A}\eta_{\boldsymbol{\sigma}}^{n},\xi_{\boldsymbol{\sigma}}^{n+1}+\xi_{\boldsymbol{\sigma}}^{n})_{\Omega}-b_h(\xi_{\boldsymbol{\sigma}}^{n+1}+\xi_{\boldsymbol{\sigma}}^{n},\eta_{\mathbf{u}}^{n+1}-\eta_{\mathbf{u}}^{n})\\&\qquad-c_h(\xi_{\boldsymbol{\sigma}}^{n+1}+\xi_{\boldsymbol{\sigma}}^{n},(\eta_{\mathbf{u}}^{n+1})^{-}-(\eta_{\mathbf{u}}^{n})^{-}).\end{aligned}\tag{5.40}$$

We then estimate the right hand sides of (5.39) and (5.40). For the first term in (5.39), Lemma 5.2 yields

$$-(\delta_{tt}\eta_{\mathbf{u}}^{n},\xi_{\mathbf{u}}^{n+1}-\xi_{\mathbf{u}}^{n-1})_{\Omega}\le C\left(h^{k+1}\|\mathbf{u}\|_{W^{2,\infty}(0,T;H^{k+1}(\Omega))}+\triangle t^2\|\boldsymbol{\sigma}\|_{W^{2,\infty}(0,T;L^2(\Omega))}\right)\|\xi_{\mathbf{u}}^{n+1}-\xi_{\mathbf{u}}^{n-1}\|_{L^2(\Omega)}.\tag{5.41}$$

For the rest of the two terms in (5.39), we apply the super-convergence property (3.4b) to obtain

$$-a_h(\eta_{\boldsymbol{\sigma}}^{n},\xi_{\mathbf{u}}^{n+1}-\xi_{\mathbf{u}}^{n-1})+c_h((\eta_{\boldsymbol{\sigma}}^{n})^{+},\xi_{\mathbf{u}}^{n+1}-\xi_{\mathbf{u}}^{n-1})\le Ch^{k+1}\|\boldsymbol{\sigma}\|_{L^{\infty}(0,T;H^{k+2}(\Omega))}\|\xi_{\mathbf{u}}^{n+1}-\xi_{\mathbf{u}}^{n-1}\|_{L^2(\Omega)}.\tag{5.42}$$

Similarly for the first term in the right hand side of (5.40), we have

$$-(\mathcal{A}\eta_{\boldsymbol{\sigma}}^{n+1}-\mathcal{A}\eta_{\boldsymbol{\sigma}}^{n},\xi_{\boldsymbol{\sigma}}^{n+1}+\xi_{\boldsymbol{\sigma}}^{n})_{\Omega}\le C\triangle th^{k+1}\|\boldsymbol{\sigma}\|_{W^{1,\infty}(0,T;H^{k+1}(\Omega))}\left(\|\xi_{\boldsymbol{\sigma}}^{n+1}\|_{\mathcal{A},\Omega}+\|\xi_{\boldsymbol{\sigma}}^{n}\|_{\mathcal{A},\Omega}\right).\tag{5.43}$$

For the remaining two terms in (5.40), by (5.35a) with the norm equivalence (3.1), we have

$$\begin{aligned}&b_h(\xi_{\boldsymbol{\sigma}}^{n+1}+\xi_{\boldsymbol{\sigma}}^{n},\eta_{\mathbf{u}}^{n+1}-\eta_{\mathbf{u}}^{n})-c_h(\xi_{\boldsymbol{\sigma}}^{n+1}+\xi_{\boldsymbol{\sigma}}^{n},(\eta_{\mathbf{u}}^{n+1})^{-}-(\eta_{\mathbf{u}}^{n})^{-})\\&\quad\le C\sqrt{\lambda+\mu}\triangle th^{k+1}\|\mathbf{u}\|_{W^{1,\infty}(0,T;H^{k+2}(\Omega))}\left(\|\xi_{\boldsymbol{\sigma}}^{n+1}\|_{\mathcal{A},\Omega}+\|\xi_{\boldsymbol{\sigma}}^{n}\|_{\mathcal{A},\Omega}\right).\end{aligned}\tag{5.44}$$

Now, we put (5.41) and (5.42) into (5.39) and put (5.43) and (5.44) into (5.40), and apply the arguments in (5.10)–(5.11) to the left side of the sum of (5.39) and (5.40). Under the notations in (5.20), this procedure yields

$$\begin{aligned}&\|\delta_t\xi_{\mathbf{u}}^{n+1}\|_{L^2(\Omega)}^2+\|\xi_{\boldsymbol{\sigma}}^{n+1}\|_{\mathcal{A},\Omega}^2-\|\delta_t\xi_{\mathbf{u}}^{n}\|_{L^2(\Omega)}^2-\|\xi_{\boldsymbol{\sigma}}^{n}\|_{\mathcal{A},\Omega}^2\\&\quad+b_h(\xi_{\boldsymbol{\sigma}}^{n+1},\xi_{\mathbf{u}}^{n+1}-\xi_{\mathbf{u}}^{n})+c_h(\xi_{\boldsymbol{\sigma}}^{n+1},(\xi_{\mathbf{u}}^{n+1})^{-}-(\xi_{\mathbf{u}}^{n})^{-})-b_h(\xi_{\boldsymbol{\sigma}}^{n},\xi_{\mathbf{u}}^{n}-\xi_{\mathbf{u}}^{n-1})\\&\quad-c_h(\xi_{\boldsymbol{\sigma}}^{n},(\xi_{\mathbf{u}}^{n})^{-}-(\xi_{\mathbf{u}}^{n-1})^{-})\\&\le C\sqrt{\lambda+\mu}\triangle t(\triangle t^2+h^{k+1})\left(\|\mathbf{u}\|_{W^{2,\infty}(0,T;H^{k+2}(\Omega))}+\|\boldsymbol{\sigma}\|_{W^{2,\infty}(0,T;H^{k+2}(\Omega))}\right)\\&\quad\cdot\left(\|\delta_t\xi_{\mathbf{u}}^{n+1}\|_{L^2(\Omega)}+\|\delta_t\xi_{\mathbf{u}}^{n}\|_{L^2(\Omega)}+\|\xi_{\boldsymbol{\sigma}}^{n+1}\|_{\mathcal{A},\Omega}+\|\xi_{\boldsymbol{\sigma}}^{n}\|_{\mathcal{A},\Omega}\right).\end{aligned}\tag{5.45}$$

Summing (5.45) from $n=1$ to any integer $M\le N$, we get

$$\begin{aligned}&\|\delta_t\xi_{\mathbf{u}}^{M+1}\|_{L^2(\Omega)}^2+\|\xi_{\boldsymbol{\sigma}}^{M+1}\|_{\mathcal{A},\Omega}^2-\|\delta_t\xi_{\mathbf{u}}^{1}\|_{L^2(\Omega)}^2-\|\xi_{\boldsymbol{\sigma}}^{1}\|_{\mathcal{A},\Omega}^2\\&\quad+b_h(\xi_{\boldsymbol{\sigma}}^{M+1},\xi_{\mathbf{u}}^{M+1}-\xi_{\mathbf{u}}^{M})+c_h(\xi_{\boldsymbol{\sigma}}^{M+1},(\xi_{\mathbf{u}}^{M+1})^{-}-(\xi_{\mathbf{u}}^{M})^{-})-b_h(\xi_{\boldsymbol{\sigma}}^{1},\xi_{\mathbf{u}}^{1}-\xi_{\mathbf{u}}^{0})\\&\quad-c_h(\xi_{\boldsymbol{\sigma}}^{1},(\xi_{\mathbf{u}}^{1})^{-}-(\xi_{\mathbf{u}}^{0})^{-})\\&\le C\sqrt{\lambda+\mu}\triangle t(\triangle t^2+h^{k+1})\left(\|\mathbf{u}\|_{W^{2,\infty}(0,T;H^{k+2}(\Omega))}\right.\\&\quad\left.+\|\boldsymbol{\sigma}\|_{W^{2,\infty}(0,T;H^{k+2}(\Omega))}\right)\cdot\sum_{i=1}^{M+1}\left(\|\delta_t\xi_{\mathbf{u}}^{i}\|_{L^2(\Omega)}+\|\xi_{\boldsymbol{\sigma}}^{i}\|_{\mathcal{A},\Omega}\right).\end{aligned}\tag{5.46}$$

Using the same arguments as in (5.13)–(5.15), for $\triangle t$ satisfying (5.7) we have

$$\begin{aligned}&|b_h(\xi_{\boldsymbol{\sigma}}^{M+1},\xi_{\mathbf{u}}^{M+1}-\xi_{\mathbf{u}}^{M})+c_h(\xi_{\boldsymbol{\sigma}}^{M+1},(\xi_{\mathbf{u}}^{M+1})^{-}-(\xi_{\mathbf{u}}^{M})^{-})|\\&\quad\le\frac{(C_i+C_t^2)^2(2+\sqrt{k(k+1)}+(k+1)(k+2))^2\triangle t^2(\lambda+\mu)}{2h^2}\|\xi_{\boldsymbol{\sigma}}^{M+1}\|_{\mathcal{A},\Omega}^2\end{aligned}$$

$$+\frac{1}{2}\frac{\|\xi_{\mathbf{u}}^{M+1}-\xi_{\mathbf{u}}^{M}\|_{L^2(\Omega)}^2}{\triangle t^2}$$
$$\leq \frac{1}{2}\left(\|\xi_{\boldsymbol{\sigma}}^{M+1}\|_{\mathcal{A},\Omega}^2+\|\delta_t\xi_{\mathbf{u}}^{M+1}\|_{L^2(\Omega)}^2\right). \tag{5.47}$$

Taking $M=0$ in (5.47), and utilizing (5.21a) and (5.21c) lead to

$$\begin{aligned} b_h(\xi_{\boldsymbol{\sigma}}^1,\xi_{\mathbf{u}}^1-\xi_{\mathbf{u}}^0)+c_h(\xi_{\boldsymbol{\sigma}}^1,(\xi_{\mathbf{u}}^1)^- -(\xi_{\mathbf{u}}^0)^-) &\leq \frac{1}{2}\left(\|\xi_{\boldsymbol{\sigma}}^1\|_{\mathcal{A},\Omega}^2+\|\delta_t\xi_{\mathbf{u}}^1\|_{L^2(\Omega)}^2\right)\\ &\leq C(\lambda+\mu)(h^{k+1}\|\mathbf{u}\|_{L^\infty(0,T;H^{k+2}(\Omega))}+(\triangle t^3h^{-1}+h^{k+1})\|\boldsymbol{\sigma}\|_{W^{1,\infty}(0,T;H^{k+1}(\Omega))})^2\\ &\leq C(\lambda+\mu)(\triangle t^2+h^{k+1})^2(\|\mathbf{u}\|_{L^\infty(0,T;H^{k+2}(\Omega))}+\|\boldsymbol{\sigma}\|_{W^{1,\infty}(0,T;H^{k+1}(\Omega))})^2, \end{aligned} \tag{5.48}$$

where we have used (5.7) again in the last inequality. Now putting (5.47) and (5.48) back into (5.46) and using (5.21a), (5.21c) again, we finally obtain the desired result. □

Finally, we have the following optimal discrete error estimates.

Theorem 5.3 *Given $\triangle t$ small enough such that (5.7) is satisfied, then for each $n\leq N$ there holds*

$$\|e_{\mathbf{u}}^n\|_{L^2(\Omega)}\leq C^*(T^2+1)\sqrt{\lambda+\mu}(\triangle t^2+h^{k+1})\left(\|\mathbf{u}\|_{W^{2,\infty}(0,T;H^{k+2}(\Omega))}+\|\boldsymbol{\sigma}\|_{W^{2,\infty}(0,T;H^{k+2}(\Omega))}\right), \tag{5.49a}$$

$$\|e_{\boldsymbol{\sigma}}^n\|_{L^2(\Omega)}\leq C^*(T+1)\sqrt{\lambda+\mu}(\triangle t^2+h^{k+1})\left(\|\mathbf{u}\|_{W^{2,\infty}(0,T;H^{k+2}(\Omega))}+\|\boldsymbol{\sigma}\|_{W^{2,\infty}(0,T;H^{k+2}(\Omega))}\right), \tag{5.49b}$$

where C^* inherits from (5.38).

Proof For simplicity's sake, we let $\gamma=C^*\sqrt{\lambda+\mu}(\triangle t^2+h^{k+1})(\|\mathbf{u}\|_{W^{2,\infty}(0,T;H^{k+2}(\Omega))}+\|\boldsymbol{\sigma}\|_{W^{2,\infty}(0,T;H^{k+2}(\Omega))})$. First of all, let's show the following estimate for every $n\leq N$:

$$\mathcal{E}_h^n\leq(n-1)\triangle t\gamma+\gamma. \tag{5.50}$$

We proceed by mathematical induction. Clearly (5.50) holds for $n=1$ because of (5.21a) and (5.21c). We assume (5.50) is true for all $n\leq M$, and we shall prove it for $n=M+1$. Using (5.38), we have

$$(\mathcal{E}_h^{M+1})^2\leq\triangle t\gamma\sum_{i=1}^{M+1}\mathcal{E}_h^i+\gamma^2\leq\triangle t\gamma\mathcal{E}_h^{M+1}+\triangle t\gamma\left(\frac{(M-1)M}{2}\triangle t\gamma+M\gamma\right)+\gamma^2. \tag{5.51}$$

Solving the quadratical inequality (5.51) for $\mathcal{E}_h^{M+1}$, we have

$$\begin{aligned}\mathcal{E}_h^{M+1}&\leq\frac{\triangle t\gamma+\sqrt{(2M^2-2M+1)\triangle t^2+4M\triangle t+4}\gamma}{2}\\ &\leq\frac{\triangle t\gamma+((2M-1)\triangle t+2)\gamma}{2}\leq M\triangle t\gamma+\gamma\end{aligned} \tag{5.52}$$

which gives (5.50) by mathematical induction. We note that (5.50) together with the optimal projection error (2.12) already yields (5.49b). Furthermore, we note that (5.50) leads to

$$\|\xi_{\mathbf{u}}^n\|_{L^2(\Omega)}-\|\xi_{\mathbf{u}}^{n-1}\|_{L^2(\Omega)}\leq\|\xi_{\mathbf{u}}^n-\xi_{\mathbf{u}}^{n-1}\|_{L^2(\Omega)}\leq(n-1)\triangle t^2\gamma+\triangle t\gamma. \tag{5.53}$$

Summing (5.53) from $n=1$ to any integer $M\leq N$, we obtain

$$\|\xi_{\mathbf{u}}^M\|_{L^2(\Omega)}-\|\xi_{\mathbf{u}}^0\|_{L^2(\Omega)}\leq\frac{M(M-1)}{2}\triangle t^2\gamma+M\triangle t\gamma\leq\frac{1}{2}T^2\gamma+T\gamma \tag{5.54}$$

which yields (5.49a) together with the optimal projection error estimate (2.12). □

Remark 5.1 We note that the fully discrete error estimates of LDG methods in the literature mainly focus on the problems with the first order time derivative [51,52,58], and their techniques can not be directly applied in the case of the second time derivative. As for the second-order wave equations, the fully discrete analysis for the leap-frog IPDG method can be found in [27], and it employs the elliptic projector induced from the coercive bilinear form of the IPDG method which is not available for the LDG method. Roughly speaking, one of the major difficulties is on the identity in (5.45) since the right hand side involves the error terms at three successive steps which can not be completely "absorbed" by the left hand side if the Young's inequality is applied, which is the essential reason we instead estimate the summation in Lemma 5.5. An implicit energy conserving temporal discretization was introduced in [30] to extend the result in [27]. Their method does not require any CFL condition depending on the mesh size, and the optimal fully discrete error estimate was also provided.

5.2 A High-Order Scheme

In this section, following [10,45,46] we describe a high-order time stepping method for the LDG scheme (2.6). Let's start with the following identity:

$$\mathbf{u}(t+\triangle t)-2\mathbf{u}(t)+\mathbf{u}(t-\triangle t)=\triangle t^2\int_{-1}^{1}(1-|\xi|)\mathbf{u}_{tt}(t+\xi\triangle t)d\xi. \tag{5.55}$$

Note that the Taylor expansion yields the following approximation

$$\mathbf{u}_{tt}(t+\xi\triangle t)\approx\mathbf{u}_{tt}(t)+\xi\triangle t\mathbf{u}_{ttt}(t)+\frac{\xi^2\triangle t^2}{2}\mathbf{u}_{tttt}(t). \tag{5.56}$$

Putting (5.56) into (5.55), we obtain $\mathbf{u}(t+\triangle t)-2\mathbf{u}(t)+\mathbf{u}(t-\triangle t)\approx\triangle t^2\mathbf{u}_{tt}(t)+\frac{\triangle t^4}{12}\mathbf{u}_{tttt}(t)$. By (5.1) we have $(\mathbf{U}_h)_{tt}(t)=\mathbf{M}^{-1}\mathbf{A}\mathbf{U}_h(t)$ and $(\mathbf{U}_h)_{tttt}(t)=\mathbf{M}^{-1}\mathbf{A}(\mathbf{U}_h)_{tt}(t)=(\mathbf{M}^{-1}\mathbf{A})^2\mathbf{U}_h(t)$. Therefore, this approximation motivates the following forth-order scheme

$$\frac{\mathbf{U}_h^{n+1}-2\mathbf{U}_h^n+\mathbf{U}_h^{n-1}}{\triangle t^2}=\mathbf{M}^{-1}\mathbf{A}\mathbf{U}_h^n+\frac{\triangle t^2}{12}(\mathbf{M}^{-1}\mathbf{A})^2\mathbf{U}_h^n. \tag{5.57}$$

Similar to (5.2), we can also rewrite (5.57) in the form of a second-order predictor step and corrector step:

$$(\mathbf{w}_h,\mathbf{v}_h)_\Omega+a_h(\boldsymbol{\sigma}_h^n,\mathbf{v}_h)-c_h((\boldsymbol{\sigma}_h^n)^+,\mathbf{v}_h)=0,\qquad\forall\mathbf{v}_h\in\mathbf{V}_h^k, \tag{5.58a}$$

$$(\mathcal{A}\boldsymbol{\sigma}_h^n,\boldsymbol{\tau}_h)_\Omega+b_h(\boldsymbol{\tau}_h,\mathbf{u}_h^n)-c_h(\boldsymbol{\tau}_h,(\mathbf{u}_h^n)^-)=0,\qquad\forall\boldsymbol{\tau}_h\in\boldsymbol{\Sigma}_h^k, \tag{5.58b}$$

with $\mathbf{w}_h=\frac{\mathbf{u}_h^*-2\mathbf{u}_h^n+\mathbf{u}_h^{n-1}}{\triangle t^2}$ and

$$\left(\mathbf{u}_h^{n+1},\mathbf{v}_h\right)_\Omega=\left(\mathbf{u}_h^*,\mathbf{v}_h\right)_\Omega+\frac{\triangle t^4}{12}\left(a_h(\tilde{\boldsymbol{\sigma}}_h^n,\mathbf{v}_h)-c_h((\tilde{\boldsymbol{\sigma}}_h^n)^+,\mathbf{v}_h)\right)=0,\qquad\forall\mathbf{v}_h\in\mathbf{V}_h^k, \tag{5.58c}$$

$$(\mathcal{A}\tilde{\boldsymbol{\sigma}}_h^n,\boldsymbol{\tau}_h)_\Omega+b_h(\boldsymbol{\tau}_h,\mathbf{w}_h)-c_h(\boldsymbol{\tau}_h,(\mathbf{w}_h)^-)=0,\qquad\forall\boldsymbol{\tau}_h\in\boldsymbol{\Sigma}_h^k, \tag{5.58d}$$

where the initial conditions are given by

$$\mathbf{u}_h^0=\mathbf{P}^-\mathbf{u}_0,\quad\text{and}\quad\mathbf{u}_h^1=\mathbf{P}^-\mathbf{u}_0+\triangle t\mathbf{P}^-\mathbf{v}_0+\frac{\triangle t^2}{2}\mathbf{P}^-\nabla\cdot\boldsymbol{\sigma}(\mathbf{u}_0)+\frac{\triangle t^3}{6}\mathbf{P}^-\nabla\cdot\boldsymbol{\sigma}(\mathbf{v}_0). \tag{5.58e}$$

Note that in (5.56) the further higher-order terms are dropped on the right hand side. If a further higher-order scheme is desired, more terms have to be kept. Besides if only the first term on the right of (5.56) is used for approximation, the second-order leap-frog scheme is obtained. The analysis for this forth-order scheme will be left for future work.

6 Numerical Examples

In this section, we present some numerical results to demonstrate the theoretical estimates above and to further investigate the long time behavior of the proposed LDG method. In addition, we shall also compare the performance of the LDG method with that of the IPDG method in some experiments. The IPDG method we have used is taken from [54]: find $\mathbf{u}_h \in \mathbf{V}_h^k$ such that

$$\int_\Omega (\mathbf{u}_h)_{tt} \cdot \mathbf{v}_h dX + \int_\Omega \boldsymbol{\sigma}(\mathbf{u}_h) : \boldsymbol{\epsilon}(\mathbf{v}_h) dX - \int_{\mathcal{E}_h} (\{\boldsymbol{\sigma}(\mathbf{u}_h)\} : [\mathbf{v}_h \otimes \mathbf{n}] + \{\boldsymbol{\sigma}(\mathbf{v}_h)\} : [\mathbf{u}_h \otimes \mathbf{n}])\, ds$$
$$+ ch^{-1} \int_{\mathcal{E}_h} (\mu [\mathbf{u}_h \otimes \mathbf{n}] : [\mathbf{v}_h \otimes \mathbf{n}] + \lambda [\mathbf{u}_h \cdot \mathbf{n}][\mathbf{v}_h \cdot \mathbf{n}])\, ds = 0, \quad \forall \mathbf{v}_h \in \mathbf{V}_h^k, \tag{6.1}$$

in which $\otimes$ denotes the Kronecker product. Here for each $e \in \mathcal{E}_h$ with the neighborhood elements K^- and K^+, we define $\{\mathbf{q}\} := \frac{1}{2}(\mathbf{q}_{K^-} + \mathbf{q}_{K^+})$, $[\mathbf{w} \otimes \mathbf{n}] := \mathbf{w}_{K^-} \otimes \mathbf{n}_{K^-} + \mathbf{w}_{K^+} \otimes \mathbf{n}_{K^+}$ and $[\mathbf{w} \cdot \mathbf{n}] := \mathbf{w}_{K^-} \cdot \mathbf{n}_{K^-} + \mathbf{w}_{K^+} \cdot \mathbf{n}_{K^+}$.

6.1 Time Stepping Constants

Note that (5.1) leads to the ODE system $(\mathbf{U}_h)_{tt}(t) = \mathbf{M}^{-1}\mathbf{A}\mathbf{U}_h(t)$. Now we let $\Lambda_{\max}$ be maximum amplitude of the eigenvalues of $\mathbf{M}^{-1}\mathbf{A}$. By the general stability analysis of ODEs, we expect $\triangle t^2 \Lambda_{\max}$ to be bounded by certain CFL constant such that the numerical scheme is stable. Then (5.7) suggests

$$\frac{h^2 \Lambda_{\max}}{\Phi(k, \lambda, \mu)} \leq \text{const.} \tag{6.2}$$

where $\Phi(k, \lambda, \mu) := (2 + \sqrt{k(k+1)} + (k+1)(k+2))^2(\lambda + \mu)$. As suggested by [3], a good choice of $\Phi(k, \lambda, \mu)$ should make the ratio in (6.2) be exactly a constant. To investigate this issue on the proposed $\Phi(k, \lambda, \mu)$, we follow the numerical experiments in [3] to compute this ratio by varying k and λ with fixing $\mu = 1$. Numerical results indicate that the scaled quantity $h^2 \Lambda_{\max}$ changes very little as h changes; so we simply focus on $h = 2/40$. In particular, in the computation for Fig. 1a and b, we first fix polynomial degree $k = 1, 2, 3$, and then compute $h^2 \Lambda_{\max}$ and $\Phi(k, \lambda, \mu)$ by varying $\lambda = 10, 20, \ldots, 100, 200, \ldots, 2000$. In Fig. 1c, we first fix $\lambda = 10, 200, 2000$ and then compute $h^2 \Lambda_{\max}$ and $\Phi(k, \lambda, \mu)$ by varying $k = 1, 2, 3, 4, 5$. In Fig. 1a and c, we can observe that the points can be approximated by a line passing through the original point. Also Fig. 1b indicates that $h^2 \Lambda_{\max} / \Phi(k, \lambda, \mu) \approx$ const. which is bounded by 1. We believe these results suggest that our theoretical estimate in (5.7) for the dependence of the stability constant on k and λ is sharp. Furthermore, our extensive numerical results on different mesh size, λ and μ also indicate $C_S = 2$ in (5.7) to guarantee the stability. Besides, we also find that it is sufficient to exclude temporal errors in computation when choosing $C_S \approx 0.1$.

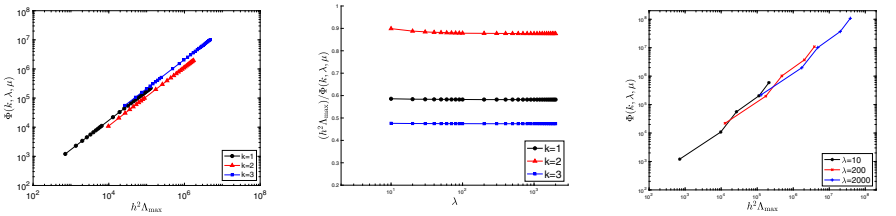

(a) $\Phi(k,\lambda,\mu)$ versus $h^2\Lambda_{\max}$ with various λ **(b)** $h^2\Lambda_{\max}/\Phi(k,\lambda,\mu)$ versus λ **(c)** $\Phi(k,\lambda,\mu)$ versus $h^2\Lambda_{\max}$ with various k

Fig. 1 Numerical estimates for the stability constants, for the example in Sect. 6.1

6.2 A Standing Wave

In this subsection, we apply the LDG method to (1.1) with the exact solution being a standing wave:

$$\mathbf{u} = \begin{bmatrix} \cos(\omega\pi t)\cos(\pi x)\sin(\pi y) \\ -\cos(\omega\pi t)\sin(\pi x)\cos(\pi y) \end{bmatrix} \tag{6.3}$$

in which the force term $\mathbf{f} = \mathbf{0}$, $\omega = \sqrt{2\mu}$, and λ and μ can be chosen arbitrarily. The domain is given by $\Omega = [-1,1]\times[-1,1]$ and the initial conditions are computed accordingly. Starting from this subsection, the numerical results for $k = 1$ are generated by the leap-frog LDG method while the results for $k = 2$ and $k = 3$ are generated by the forth-order scheme introduced in Sect. 5.2.

First of all, we fix $\lambda = 10$, $\mu = 1$, and $T = 1$. Then we compute the solution errors for $k = 1, 2, 3$ in terms of the L^2 norm for $\mathbf{u}$ and the energy norm $\|\cdot\|_{\mathcal{A},\Omega}$ for $\boldsymbol{\sigma}$. We also compare the errors for the initial conditions constructed by the Gauss-Radau projection (5.2c) and the standard L^2 projection. The results at $t = 0.5$ and $t = 1$ are presented in Figs. 2 and 3 , and the corresponding convergence rates are estimated and indicated on the graph. From Fig. 2 for $\mathbf{u}$, we can observe that both the solutions computed by the initial conditions with the Gauss-Radau projection and the L^2 projection converge optimally. We can also see that the errors from the Gauss-Radau projection are slightly smaller than the errors from the L^2 projection, and this difference becomes gradually large as the time evolves. However the Fig. 3 indicates that the solution errors of the stress $\boldsymbol{\sigma}$ by the Gauss-Radau projection are much smaller than those by the L^2 projection. In addition, while the convergence rates for the Gauss-Radau projection are optimal which agrees with the analysis in the previous sections, the convergence rates for the L^2 projection are only suboptimal, i.e., h^k if the $\mathbb{Q}^k$ polynomial spaces are used. This phenomenon was also observed in [10] for the energy conserving LDG method applied to the scalar second-order wave equations. We also note that the authors in [1] actually have proved the h^k convergence rate for the energy-conserving LDG method applied to elastodynamics system if the Lagrange interpolation is used for constructing initial conditions. The essential difference in the analysis is the employment of trace inequalities on element edges which causes the loss of accuracy. However some earlier studies [9,33] on LDG methods suggest that the choice of the initial conditions do not have much effect on the solution errors. We expect that this may be due to the energy conservation property of our method which can not dissipate the initial error.

Next, we perform the same computation but with the approximation space $\mathbb{P}^k$ instead of $\mathbb{Q}^k$, and compare their numerical results in Figs. 4, 5. This experiment is to test whether the

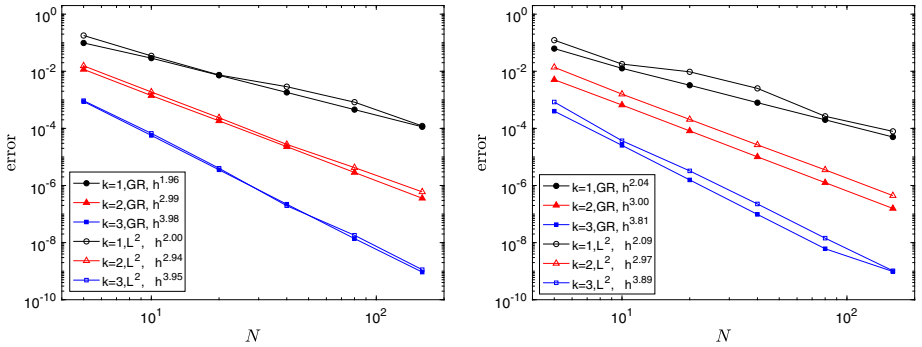

Fig. 2 Comparison of errors for $\mathbf{u}$ of the standing wave example between initial conditions constructed by L^2 and Gauss-Radau projections: $t = 0.5$ (left) and $t = 1$ (right)

standard polynomial space $\mathbb{P}^k$ can achieve the same accuracy and convergence order, since it is just a subspace of $\mathbb{Q}^k$ with fewer degrees of freedom and can make the computation more efficient. Figure 4 shows that the errors of the displacement $\mathbf{u}$ using $\mathbb{P}^k$ space can converge optimally but they are much larger than those using $\mathbb{Q}^k$, and this difference becomes more significant as the degree k increases. Furthermore, the comparison for the stress $\boldsymbol{\sigma}$ is presented in Fig. 5, where one can observe that the errors using $\mathbb{P}^k$ are not only much larger than those using $\mathbb{Q}^k$, but also loss order of convergence. In particular, while the errors of $\mathbb{Q}^1$ and $\mathbb{P}^1$ have almost the same numerical behavior, the errors of $\mathbb{P}^2$ and $\mathbb{P}^3$ loss about 0.7 and 1 order of convergence, respectively, i.e., the numerical results of $\mathbb{P}^k$ also become worse as k increases. We emphasize that this actually agrees with the observation in [10] for the second order acoustic wave equations.

Furthermore, we also investigate the numerical behavior of the proposed LDG method as the Young's module $\nu \to \frac{1}{2}$, i.e., the ratio of the Lamé parameter $\lambda/\mu \to \infty$, and use the results of the standard IPDG method as the reference for comparison. Note that the exact solution (6.3) only depends on μ, and thus to simplify the investigation, we fix $\mu = 1$ and vary $\lambda = 2, 2^2, \ldots, 2^{13}$. The numerical results generated at $t = 1$ are presented in Figs. 6 and 7 . We clearly observe that the errors of $\mathbf{u}$ for the LDG method are independent with the growth of λ, while the errors of the IPDG method grow and are much larger than those of the LDG method when $\lambda = 2^{13}$. As for $\boldsymbol{\sigma}$, the errors of both the LDG and IPDG methods grow as λ increases, but the errors of the LDG method are much smaller than those of the IPDG method. We emphasize that it is particularly critical to compute more accurate stress tensor for the linear elasticity system which shows the advantage of the LDG method. In addition, the dashed reference lines in Fig. 7 indicate the growth rate $\lambda^{1/2}$ as suggested by the theoretical estimate in Theorem 5.3. We can see that the numerical results match this growth rate quite well; hence we believe the dependence on λ for the error of $\boldsymbol{\sigma}$ in Theorem 5.3 is sharp. However Theorem 5.3 also indicates the dependence for the error of $\mathbf{u}$ should be still $\lambda^{1/2}$, and this is actually worse than the numerical results. How to prove this independence shown by Fig. 6 is an interesting topic left for future research.

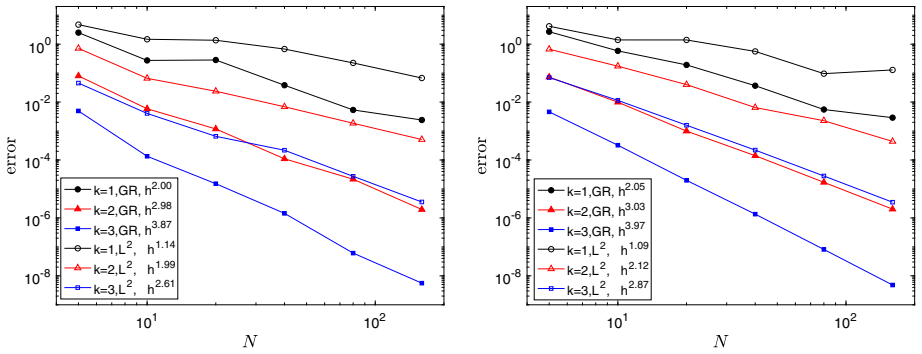

Fig. 3 Comparison of errors for $\boldsymbol{\sigma}$ of the standing wave example between initial conditions constructed by L^2 and Gauss-Radau projections: $t = 0.5$ (left) and $t = 1$ (right)

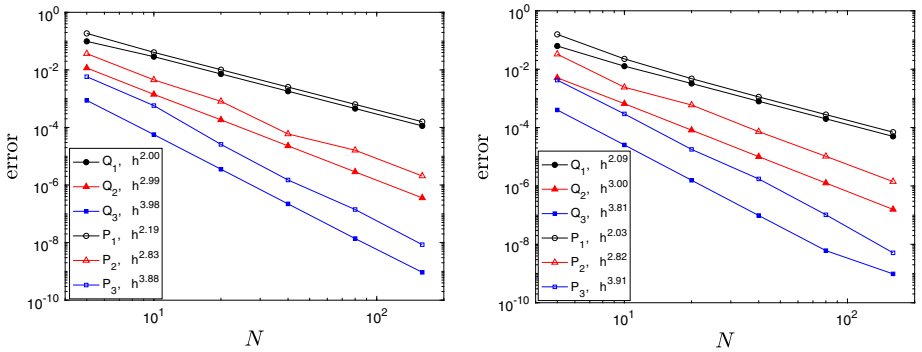

Fig. 4 Comparison of errors for $\mathbf{u}$ of the standing wave example between $\mathbb{Q}^k$ and $\mathbb{P}^k$ approximation spaces: $t = 0.5$ (left) and $t = 1$ (right)

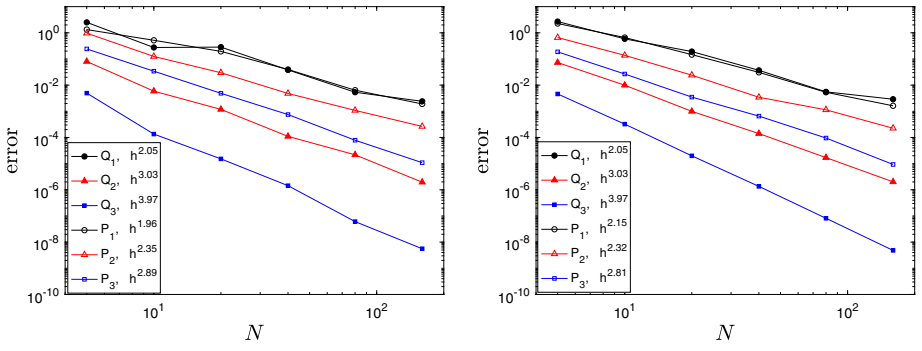

Fig. 5 Comparison of errors for $\boldsymbol{\sigma}$ of the standing wave example between $\mathbb{Q}^k$ and $\mathbb{P}^k$ approximation spaces: $t = 0.5$ (left) and $t = 1$ (right)

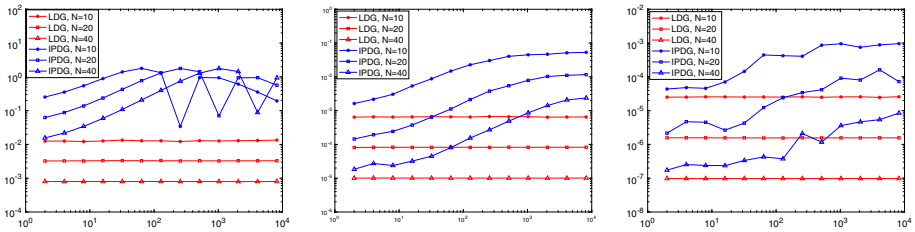

Fig. 6 Errors of LDG and IPDG methods for $\mathbf{u}$ versus increasing λ of the standing wave example: $k = 1$ (left), $k = 2$ (middle) and $k = 3$ (right)

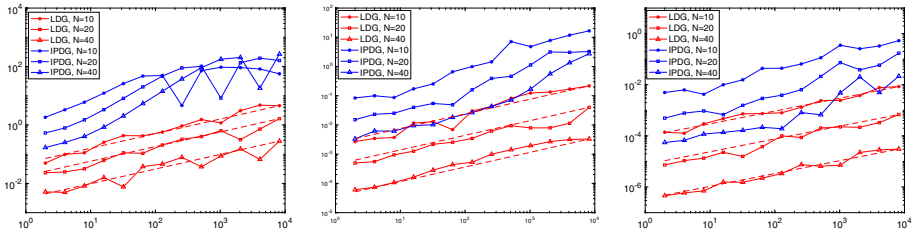

Fig. 7 Errors of LDG and IPDG methods for $\boldsymbol{\sigma}$ versus increasing λ of the standing wave example: $k = 1$ (left), $k = 2$ (middle) and $k = 3$ (right)

6.3 A Traveling Wave

In this subsection, we use the following traveling wave function as an example to investigate the behavior of the LDG method in long time simulation:

$$\mathbf{u} = \begin{bmatrix} -\cos(\omega\pi t + \kappa\pi x)\sin(\kappa\pi y) \\ -\sin(\omega\pi t + \kappa\pi x)\cos(\kappa\pi y) \end{bmatrix} \tag{6.4}$$

in which the force term $\mathbf{f} = \mathbf{0}$, $\omega = \sqrt{2\kappa^2\lambda + 4\kappa^2\mu}$, and κ, λ, μ can be chosen arbitrarily. According to our extensive numerical experiments, larger frequency κ gives larger long time errors. Here we focus on $\kappa = 3$. We also consider the computation domain $\Omega = [-1, 1] \times [-1, 1]$, and the initial conditions are computed accordingly.

The numerical results are presented in Figs. 8 and 9 . From the first and third plots in these two figures, we can clearly observe that the errors of the IPDG method for both $\mathbf{u}$ and $\boldsymbol{\sigma}$ are about 100 times larger than those of the LDG method at some long time point, such as $t \geq 100$. Furthermore, the second and forth plots in Figs. 8 and 9 indicate that the growth of errors are all linear with respect to time for both IPDG and LDG methods. This actually agrees with our estimates in Theorems 5.3 and 4.2 for $\boldsymbol{\sigma}$ but not for $\mathbf{u}$. We also emphasize the slope of the LDG method is much smaller than the one of the IPDG method. In particular, when $k = 3$, both the errors of $\mathbf{u}$ and $\boldsymbol{\sigma}$ are actually almost independent of the evolution for the LDG method, namely they stay almost unchanged. The related sharp analysis for the growth of the errors of $\mathbf{u}$ with respect to time needs future research. In addition, we plot the wave shape in Fig. 10 for $y = 0.6$ and $y = 0.8$ at $T = 1000$ when $k = 2$. We note that there is apparently some visible dispersion error for the IPDG method, but the wave of the LDG method matches with the exact solution very well. All these computations indeed show the advantages of the LDG methods in long time simulation.

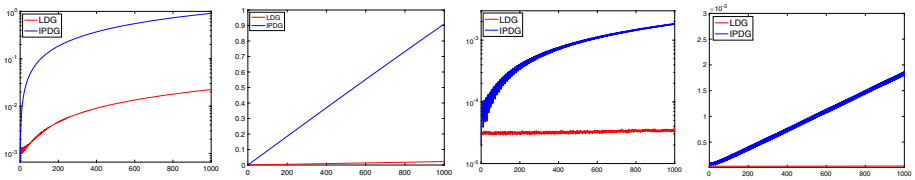

Fig. 8 Long time errors for $\mathbf{u}$ of the traveling wave example: left two plots are for $k = 2$ where the first one uses log-scale for the y-axis and right two plots are for $k = 3$ where the first one uses log-scale for the y-axis

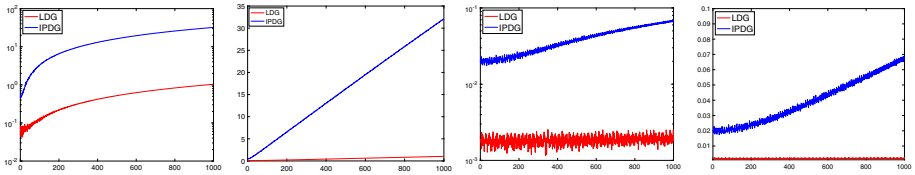

Fig. 9 Long time errors for $\boldsymbol{\sigma}$ of the traveling wave example: left two plots are for $k = 2$ where the first one uses log-scale for the y-axis and right two plots are for $k = 3$ where the first one uses log-scale for the y-axis

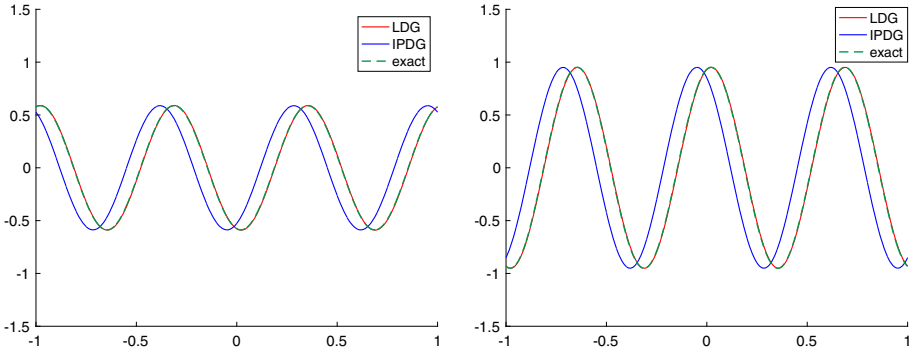

Fig. 10 Wave shape of $\mathbf{u}$ of the traveling wave example, at $y = 0.6$ (left) and $y = 0.8$ (right) for $k = 2$ when $t = 1000$

7 Conclusion Remarks

In this paper, we have presented and analyzed an LDG method to solve elastic wave propagation problems. The proposed method has the features to conserve the energy exactly through the dynamics and, at the same, to achieve optimal $O(h^{k+1} + \triangle t^2)$ convergence rates with the $\mathbb{Q}^k$ spatial discretization and leap-frog temporal discretization. Numerical experiments demonstrate that the proposed method has several advantages including the exact energy conservation, slow-growing errors in long time simulation, and subtle dependence on the first Lamé parameter λ. Numerical comparison with the results of IPDG methods also indicates the effectivity of the proposed method in the long time simulation. Note that the proof of the optimal error estimate requires Cartesian meshes which may not be applicable for complicated boundary or interface geometry. Recently, optimal error estimate of DG methods with generalized fluxes for wave equations on unstructured meshes was carried out by one of the

authors in [48], and we will leave the detailed study of its extension to elastodynamics to a future work.

Data Availability Statement The datasets generated during and/or analyzed during the current study are available from the corresponding author on reasonable request.

References

1. Antonietti, P.F., de Dios, B.A., Mazzieri, I., Quarteroni, A.: Stability analysis of discontinuous galerkin approximations to the elastodynamics problem. J. Sci. Comput. **68**(1), 143–170 (2016)
2. Antonietti, P.F., Mazzieri, I.: High-order discontinuous Galerkin methods for the elastodynamics equation on polygonal and polyhedral meshes. Comput. Methods Appl. Mech. Eng. **342**, 414–437 (2018)
3. Appelö, D., Hagstrom, T.: An energy-based discontinuous Galerkin discretization of the elastic wave equation in second order form. Comput. Methods Appl. Mech. Eng. **338**, 362–391 (2018)
4. Arnold, D.N., Lee, J.J.: Mixed methods for elastodynamics with weak symmetry. SIAM J. Numer. Anal. **52**(6), 2743–2769 (2013)
5. Bassi, F., Rebay, S.: A high-order accurate discontinuous finite element method for the numerical solution of the compressible Navier-Stokes equations. J. Comput. Phys. **131**(2), 267–279 (1997)
6. Bécache, E., Joly, P., Tsogka, C.: A new family of mixed finite elements for the linear elastodynamic problem. SIAM J. Numer. Anal. **39**(6), 2109–2132 (2002)
7. Bona, J.L., Chen, H., Karakashian, O.A., Xing, Y.: Conservative discontinuous Galerkin methods for the generalized Korteweg-de Vries equation. Math. Comput. **82**, 1401–1432 (2013)
8. Castillo, P., Cockburn, B., Perugia, I., Schötzau, D.: An a priori error analysis of the local discontinuous Galerkin method for elliptic problems. SIAM J. Numer. Anal. **38**(5), 1676–1706 (2000)
9. Cheng, Y., Shu, C.-W.: Superconvergence of discontinuous Galerkin and local discontinuous Galerkin schemes for linear hyperbolic and convection-diffusion equations in one space dimension. SIAM J. Numer. Anal. **47**(6), 4044–4072 (2010)
10. Chou, C.-S., Shu, C.-W., Xing, Y.: Optimal energy conserving local discontinuous Galerkin methods for second-order wave equation in heterogeneous media. J. Comput. Phys. **272**, 88–107 (2014)
11. Chung, E.T., Du, J., Lam, C.Y.: Discontinuous Galerkin methods with staggered hybridization for linear elastodynamics. Comput. Math. Appl. **74**(6), 1198–1214 (2017)
12. Chung, E.T., Engquist, B.: Optimal discontinuous Galerkin methods for wave propagation. SIAM J. Numer. Anal. **44**(5), 2131–2158 (2006)
13. Cockburn, B., Zhixing, F., Hungria, A., Ji, L., Sanchez, M.A., Sayas, F.-J.: Stormer-numerov HDG methods for acoustic waves. J. Sci. Comput. **75**, 597–624 (2018)
14. Cockburn, B., Kanschat, G., Perugia, I., Schötzau, D.: Superconvergence of the local discontinuous Galerkin method for elliptic problems on cartesian grids. SIAM J. Numer. Anal. **39**(1), 264–285 (2001)
15. Cockburn, B., Shu, C.-W.: TVB Runge-Kutta local projection discontinuous Galerkin finite element method for conservation laws ii: General framework. Math. Comput. **52**(186), 411–435 (1989)
16. Cockburn, B., Shu, C.-W.: The local discontinuous Galerkin method for time-dependent convection-diffusion systems. SIAM J. Numer. Anal. **35**(6), 2440–2463 (1998)
17. De Basabe, J.D., Sen, M.K., Wheeler, M.F.: The interior penalty discontinuous Galerkin method for elastic wave propagation: grid dispersion. Geophys. J. Int. **175**(1), 83–93 (2008)
18. Demkowicz, L., Oden, J.T.: Application of hp-adaptive BE/FE methods to elastic scattering. Comput. Methods Appl. Mech. Eng. **133**(3), 287–317 (1996)
19. Di Pietro, D.A., Nicaise, S.: A locking-free discontinuous Galerkin method for linear elasticity in locally nearly incompressible heterogeneous media. Appl. Numer. Math. **63**, 105–116 (2013)
20. Dong, B., Shu, C.-W.: Analysis of a local discontinuous Galerkin method for linear time-dependent fourth-order problems. SIAM J. Numer. Anal. **47**(5), 3240–3268 (2009)
21. Douglas Jr., J., Gupta, C.P.: Superconvergence for a mixed finite element method for elastic wave propagation in a plane domain. Numer. Math. **49**, 189–202 (1986)
22. Du, S., Sayas, F.-J.: New analytical tools for HDG in elasticity, with applications to elastodynamics. Math. Comput. **89**, 1745–1782 (2020)
23. Etienne, V., Chaljub, E., Virieux, J., Glinsky, N.: An hp-adaptive discontinuous Galerkin finite-element method for 3-D elastic wave modelling. Geophys. J. Int. **183**(2), 941–962 (2010)
24. Falk, R.S., Richter, G.R.: Explicit finite element methods for symmetric hyperbolic equations. SIAM J. Numer. Anal. **36**(3), 935–952 (1999)

25. Fernandez, P., Christophe, A., Terrana, S., Nguyen, N.C., Peraire, J.: Hybridized discontinuous Galerkin methods for wave propagation. J. Sci. Comput. **77**(3), 1566–1604 (2018)
26. García, C., Gatica, G.N., Meddahi, S.: A new mixed finite element method for elastodynamics with weak symmetry. J. Sci. Comput. **72**(3), 1049–1079 (2017)
27. Grote, M.J., Schötzau, D.: Optimal error estimates for the fully discrete interior penalty dg method for the wave equation. J. Sci. Comput. **40**(1), 257–272 (2009)
28. Guo, K., Acosta, S., Chan, J.: A weight-adjusted discontinuous Galerkin method for wave propagation in coupled elastic–acoustic media. J. Comput. Phys. **418**, 109632 (2020)
29. Guo, R., Lin, T., Lin, Y.: Recovering elastic inclusions by shape optimization methods with immersed finite elements. J. Comput. Phys. **404**, 109123 (2020)
30. Han, W., He, L., Wang, F.: Optimal order error estimates for discontinuous Galerkin methods for the wave equation. J. Sci. Comput. **78**(1), 121–144 (2019)
31. Hesthaven, J.S., Warburton, T.: *Nodal discontinuous Galerkin methods*, volume 54 of *Texts in Applied Mathematics*. Springer, New York. Algorithms, analysis, and applications (2008)
32. Huang, Y., Liu, H., Yi, N.: A conservative discontinuous Galerkin method for the Degasperis-Procesi equation. Methods Appl. Anal. **21**, 67–90 (2014)
33. Hufford, C., Xing, Y.: Superconvergence of the local discontinuous Galerkin method for the linearized korteweg-de vries equation. J. Comput. Appl. Math. **255**, 441–455 (2014)
34. Hughes, T.J.R., Hulbert, G.M.: Space-time finite element methods for elastodynamics: formulations and error estimates. Comput. Methods Appl. Mech. Eng. **66**(3), 339–363 (1988)
35. Joly, P.: Variational methods for time-dependent wave propagation problems. Springer, Berlin, Heidelberg (2003)
36. Komatitsch, D., Vilotte, J.-P., Vai, R., Castillo-Covarrubias, J.M., Sánchez-Sesma, F.J.: The spectral element method for elastic wave equations–application to 2-d and 3-d seismic problem. Int. J. Numer. Methods Eng. **45**(9), 1139–1164 (1999)
37. Li, X., Sun, W., Xing, Y., Chou, C.-S.: Energy conserving local discontinuous Galerkin methods for the improved Boussinesq equation. J. Comput. Phys. **401**, 109002 (2020)
38. Liang, X., Khaliq, A.Q.M., Xing, Y.: Fourth order exponential time differencing method with local discontinuous Galerkin approximation for coupled nonlinear Schrodinger equations. Commun. Comput. Phys. **17**, 510–541 (2015)
39. Liu, H., Xing, Y.: An invariant preserving discontinuous Galerkin method for the Camassa–Holm equation. SIAM J. Sci. Comput. **38**, A1919–A1934 (2016)
40. Matuszyk, P.J., Demkowicz, L.F., Torres-Verdin, C.: Solution of coupled acoustic-elastic wave propagation problems with anelastic attenuation using automatic hp-adaptivity. Comput. Methods Appl. Mech. Eng. **213–216**, 299–313 (2012)
41. Meng, X., Shu, C.-W., Boying, W.: Optimal error estimates for discontinuous Galerkin methods based on upwind-biased fluxes for linear hyperbolic equations. Math. Comput. **85**(299), 1225–1261 (2016)
42. Nguyen, N.C., Peraire, J., Cockburn, B.: High-order implicit hybridizable discontinuous Galerkin methods for acoustics and elastodynamics. J. Comput. Phys. **230**(10), 3695–3718 (2011)
43. Rivière, B., Shaw, S., Wheeler, M.F., Whiteman, J.R.: Discontinuous Galerkin finite element methods for linear elasticity and quasistatic linear viscoelasticity. Numer. Math. **95**(2), 347–376 (2003)
44. Schuster, G.T.: Seismic inversion. Society of Exploration Geophysicists, Houston (2017)
45. Shubin, G.R., Bell, J.B.: A modified equation approach to constructing fourth order methods for acoustic wave propagation. SIAM J. Sci. Stat. Comput. **8**(2), 135–151 (1987)
46. Sjögreen, B., Petersson, N.A.: A fourth order accurate finite difference scheme for the elastic wave equation in second order formulation. J. Sci. Comput. **52**(1), 17–48 (2012)
47. Sticko, S., Kreiss, G.: Higher order cut finite elements for the wave equation. J. Sci. Comput. **80**(3), 1867–1887 (2019)
48. Sun, Z., Xing, Y.: Optimal error estimates of discontinuous Galerkin methods with generalized fluxes for wave equations on unstructured meshes. Math. Comput. (in press) https://doi.org/10.1090/mcom/3605
49. Terrana, S., Vilotte, J.P., Guillot, L.: A spectral hybridizable discontinuous Galerkin method for elastic-acoustic wave propagation. Geophys. J. Int. **213**(1), 574–602 (2017)
50. Virieux, J.: P-sv wave propagation in heterogeneous media: velocity-stress finite-difference method. Geophysics **51**(4), 889–901 (1986)
51. Wang, H., Wang, S., Zhang, Q., Shu, C.-W.: Local discontinuous Galerkin methods with implicit–explicit time-marching for multi-dimensional convection-diffusion problems. ESAIM Math. Model. Numer. Anal. **50**(4), 1083–1105 (2016)
52. Wang, H., Zhang, Q.: Error estimate on a fully discrete local discontinuous Galerkin method for linear convection–diffusion problem. J. Comput. Math. **31**(3), 283–307 (2013)

53. Warburton, T., Hesthaven, J.S.: On the constants in hp-finite element trace inverse inequalities. Comput. Methods Appl. Mech. Eng. **192**(25), 2765–2773 (2003)
54. Wihler, T.P.: Locking-free adaptive discontinuous Galerkin FEM for linear elasticity problems. Math. Comput. **75**(255), 1087–1102 (2006)
55. Wilcox, L.C., Stadler, G., Burstedde, C., Ghattas, O.: A high-order discontinuous Galerkin method for wave propagation through coupled elastic–acoustic media. J. Comput. Phys. **229**(24), 9373–9396 (2010)
56. Xing, Y., Chou, C.-S., Shu, C.-W.: Energy conserving local discontinuous Galerkin methods for wave propagation problems. Inverse Problems Imag. **7**, 967 (2013)
57. Yan, X., Shu, C.-W.: Local discontinuous Galerkin methods for high-order time-dependent partial differential equations. Commun. Comput. Phys. **7**, 1–46 (2010)
58. Zhang, Q., Shu, C.-W.: Stability analysis and a priori error estimates of the third order explicit Runge–Kutta discontinuous Galerkin method for scalar conservation laws. SIAM J. Numer. Anal. **48**(3), 1038–1063 (2010)